



# Synthesis and evaluation of 5-(Phenyl)-4H-1,2,4-triazole-3-thiol as Corrosion Inhibitor for Mild Steel in 0.5M H<sub>2</sub>SO<sub>4</sub> and its synergistic effect with potassium iodide

S. Messikh<sup>1</sup>, R. Salhi<sup>1\*</sup>, O. Benali<sup>2</sup>, H. B. Ouici<sup>3</sup> and N. Gherraf<sup>4</sup>

<sup>1</sup>\*Department of Chemistry, Faculty of Exact Sciences, University Mentouri Brothers, Constantine, Algeria, <sup>2</sup>Department of Biology, Faculty of Science and Technology, University Moulay Tahar, Saïda, Algeria, <sup>3</sup>Department of Chemistry, Faculty of Science and Technology, University Moulay Tahar, Saïda, Algeria and <sup>4</sup>Laboratory of Natural Resources and Management of Sensitive Environments, Larbi ben M'hidi University, Oum El Bouaghi, 04000, Algeria

## Abstract

The corrosion inhibition by 5-(Phenyl)-4H-1,2,4-triazole-3-thiol (PTT) on mild steel in 0.5M H<sub>2</sub>SO<sub>4</sub> solution has been investigated by weight loss, electrochemical impedance spectroscopy (EIS) and potentiodynamic polarization techniques at various concentrations and temperatures. The results obtained revealed that this compound performed excellently as corrosion inhibitor for mild steel in 0.5M H<sub>2</sub>SO<sub>4</sub> solution. It was found that the inhibition efficiency increased with inhibitor concentration reached a maximum of 91.6 % at 0.5 mM. The addition of potassium iodide to PTT in solution increased the inhibition efficiency of this latter. A synergistic effect was observed between KI and inhibitor with optimum of concentration of 0.5 mM/PTT + 0.2% potassium iodide. Potentiodynamic polarization studies have shown that PTT inhibitor acts as a mixed-type inhibitor retarding the anodic and cathodic corrosion reactions with predominant effect on the cathodic reaction. Adsorption of inhibitor alone or in combination with potassium iodide on the metal surface obeyed the Langmuir adsorption isotherm. The effect of temperature on the inhibition efficiency was also determined, some thermodynamic parameters such as apparent activation energy and adsorption free energy have been calculated and discussed. Results obtained with different methods are in good agreement. Scanning electron microscopy (SEM) study confirmed that the inhibition of corrosion of mild steel is through adsorption of the extract molecules on surface of metal. Quantum chemical parameters were also calculated to characterize adsorption mechanism. Acceptable correlations were obtained between experimental (inhibition efficiencies,  $\Delta G_{ads}$ ,  $E_a$ ) and quantum calculation parameters (dipole moment,  $E_{HOMO}$ ,  $E_{LUMO}$ ). The high inhibition efficiency was declined in terms of strongly adsorption of protonated inhibitor molecules on the metal surface and forming a protective film.

Originality/value—Electrochemical techniques have been used for the first time to study synergistic effect of PTT inhibitor and potassium iodide on inhibition of corrosion of mild steel in 0.5M H<sub>2</sub>SO<sub>4</sub> solution. The results suggest that the mixture (PTT + KI) could find practical application in corrosion control in aqueous acidic environment.

The effect of molecular structure on the inhibition efficiency has been investigated by quantum chemical calculations. The electronic properties of inhibitor were calculated and are discussed. The theoretical results were found to be consistent with the experimental data reported.

**Keywords:** Mild steel; Corrosion inhibitor; 1,2,4-triazole; H<sub>2</sub>SO<sub>4</sub> solution; EIS; Tafel polarization; SEM; Density functional theory

Full length article \*Corresponding Author, e-mail: [Salhiram@yahoo.fr](mailto:Salhiram@yahoo.fr)

## 1. Introduction

Mild steel is one of the important materials used in various industries due to its excellent mechanical properties and low cost. The study of carbon steel corrosion phenomena has become important particularly in acidic media because of the increased industrial applications of acid solutions. One of the most common, effective and

economic method to protect metals against corrosion is use of organic compounds (containing heteroatoms having higher basicity and electron density like nitrogen, oxygen and sulphur) as corrosion inhibitors [1-10]. Compounds containing hetero atoms in their aromatic or long carbon chain are capable of being adsorbed on the metal surface and can protect the metal against corrosion. For this class of

compounds, the presence of hetero atoms (nitrogen, sulphur, oxygen and even selenium and phosphorous) and  $\pi$ -electrons in their double or triple bonds have been found to help the adsorption of the metal. The exiting data reveal that most organic inhibitors act by adsorption on the metal surface [11-13]. These inhibitors are usually adsorbed on the metal surface by the formation of a coordinate covalent bond (chemical adsorption) or the electrostatic interaction between the metal and inhibitor (physical adsorption). This adsorption produces a uniform film on the metal surface, which reduces or prevents contact with the corrosive medium. Because organic inhibitors act by adsorption on the metal surface, the efficiency of these compounds depends strongly on their ability to form complexes with the metal. Both  $\pi$  electrons and polar groups containing sulfur, oxygen and/or nitrogen are fundamental characteristics of this type of inhibitor. The polar functional groups are usually considered the chelation center for chemical adsorption. This adsorption is influenced by the nature and surface charge of metal, the type of aggressive electrolyte and the chemical structure of inhibitors [4, 14-27]. Triazole and its derivatives have been widely studied [28-32] in experimental and theoretical researches. Triazole and triazole-type compounds containing nitrogen, sulphur, and heterocycle on the corrosion inhibition of metal in acidic media have attracted more attention because of their excellent corrosion inhibition performance [33-39]. They are not only used against corrosion but also preferred for biological activities such as antiviral, antibacterial, antifungal and antituberculous. It is known that most of them were reported as green inhibitor due to environmentally friendly effects [28]. The majority of corrosion inhibition studies of steel in  $H_2SO_4$  media using different organic compounds showed less inhibition efficiency than in HCl medium. Interestingly, like HCl,  $H_2SO_4$  is also used in large quantity for removing undesirable scale and rust formed on steel surface especially in boilers, heat exchangers and oil refineries. Hence in these cases the inhibition efficiency of added inhibitor enhanced to greater than 95% by the addition of halide ions especially iodide ions [40]. Synergism is an effective method to improve the inhibitive action of an inhibitor in presence of another substance in corrosive medium and to decrease amount of usage. The addition of halide salts to some inhibitor solution results in synergistic effect. Recently, several studies have been reported to explain role of synergism on corrosion inhibition mechanism of steel in sulphuric acid ( $H_2SO_4$ ) medium [41-46]. This synergism is due to increased surface coverage as a result of ion-pair interactions between organic cation and halide anion. The halide ions present in an inhibiting solution adsorb on corroding electrode surface by creating oriented dipoles and facilitates the adsorption of inhibitor cations on the dipoles [42]. The synergism between an inhibitor and other ions

such as iodide has been extensively studied by many authors [47-49].

In the present investigation, the synergistic influence of iodide ions in the performance of PTT as a corrosion inhibitor of carbon steel in 0.5M  $H_2SO_4$  has been systematically studied by weight loss measurements, potentiodynamic polarization studies and impedance measurements. The surface morphology of inhibited mild steel was analyzed by scanning electron microscope technology SEM. DFT methods have been used to analyze the characteristics of the inhibitor/surface mechanism and to describe the structural nature of the inhibitor in the corrosion process [12]. Presently, quantum chemical calculations and molecular simulation studies have been proved to be a very useful tool for studying the mechanism of corrosion inhibition. Quantum chemical parameters such as energy of molecular orbitals, highest occupied molecular orbital (HOMO) and lowest unoccupied molecular orbital (LUMO), energy gap ( $\Delta E$ ) between HOMO and LUMO, dipole moment, electronic chemical potential ( $\mu$ ) are directly related to the performance of inhibitors. Results are reported and discussed [50-54].

## 2. Experimental Section

### 2.1. Materials and Sample Preparation

The triazole derivative namely PTT has been synthesized in our laboratory as shown in Fig. 1 via aromatic carboxylic acid hydrazide intermediate [55, 56]. The aromatic carboxylic acid is first esterified in the presence of concentrated  $H_2SO_4$  and absolute ethanol. The corresponding acid ester is then treated with 80% hydrazine hydrate in the presence of absolute ethanol as solvent that resulted in the formation of corresponding carboxylic acid hydrazide in equimolar proportions. The resulting hydrazide is treated with potassium thiocyanate in acidic medium which resulted in the formation of thiosemicarbazide and the yields were quantitative. Cyclization of the thiosemicarbazide in the presence of NaOH resulted in the formation of the corresponding carboxylic acid-1,2,4-triazole-3-thiol derivative [57]. The obtained compound was purified and analyzed by IR and NMR spectroscopies before use.

The aggressive solutions of 0.5M  $H_2SO_4$  were prepared by dilution of analytical reagent grade 98%  $H_2SO_4$  with double-distilled water. The concentration range of the inhibitor employed was 0.1 to 0.5 mM, and the solution in the absence of inhibitor was taken as blank for comparison.

The blend inhibitor, PTT+KI, solutions were prepared by adding specified amount of AR grade KI to PTT- $H_2SO_4$  solution. All experiments were performed in aerated and stagnant solutions.

Mild steel specimens containing  $C \leq 0.214\%$ ,  $Si \leq 0.237\%$ ,  $Mn \leq 1.054\%$ ,  $S \leq 0.006\%$ ,  $P \leq 0.015\%$ ,  $Ni \leq 0.066\%$ ,  $Cu \leq 0.059\%$  and the remainder iron was used as the working electrode for all studies. Prior to all

measurements, the samples were mechanically abraded with 220, 400, 800, 1200 and 2400 emery paper, degreased with ethanol, washed with double-distilled water and dried at room temperature and stored in vacuum desiccator before immersion in the test solution.

## 2.2. Methods of Study

### 2.2.1. Weight Loss Measurements

The weight loss experiments were carried out using cylindrical mild steel specimens (98%) with exposed total area of 2.58 cm<sup>2</sup>. Mild steel specimens were polished, washed and dried, then weighted and suspended in a 50 ml solution of 0.5 M H<sub>2</sub>SO<sub>4</sub> for 1 h in the absence and the presence of various amounts of inhibitor (PTT) and KI. After the elapsed time, the specimens were taken out, washed, dried and weighed accurately. The experimental studies were performed at temperature range of 298 K to 323 K. All weight loss measurements were performed in triplicates. The inhibition efficiency was evaluated from the calculated corrosion rate (CR) using the Eq. (1) [58, 59]:

$$IE (\%) = \frac{CR_0 - CR_{inh}}{CR_0} \times 100 \quad (1)$$

Where CR<sub>0</sub> and CR<sub>inh</sub> are the corrosion rates of steel (mg cm<sup>-2</sup>h<sup>-1</sup>) in absence and in presence of inhibitors, respectively.

### 2.2.2. Electrochemical Measurements

Electrochemical experiments were carried out in a glass cell (CEC/TH-Radiometer) with a capacity of 500 ml. A platinum electrode and a saturated calomel electrode (SCE) were used as a counter electrode and a reference electrode. The working electrode (WE) was in the form of a disc cut from mild steel under investigation and was embedded with epoxy steel resin to offer an exposed surface area of 1 cm<sup>2</sup>. Electrochemical impedance spectroscopy (EIS) and potentiodynamic polarization were conducted in an electrochemical measurement system (VoltaLab40) which comprises a PGZ301 potentiostat, a personal computer and Voltmaster 4 and Ec-Lab software. The potentiodynamic current–potential curves were recorded by changing the electrode potential automatically from – 800 to – 200 mV with scanning rate of 0.5 mV s<sup>-1</sup>. The polarization resistance measurements were performed by applying a controlled potential scan over a small range typically 15 mV with respect to E<sub>corr</sub>. All experiments were carried out in freshly prepared solution at 303 K. The AC impedance measurements were performed at corrosion potentials (E<sub>corr</sub>) over a frequency range of 100 kHz – 10 mHz, with a signal amplitude perturbation of 5 mV. Nyquist plots were obtained. The inhibition efficiency was evaluated from the measured I<sub>corr</sub> values using the Eq. (2) [59, 60]:

$$IE (\%) = \frac{I_{corr(0)} - I_{corr(inh)}}{I_{corr(0)}} \times 100 \quad (2)$$

Where I<sub>corr(0)</sub> and I<sub>corr(inh)</sub> are the corrosion current densities in the absence and presence of the inhibitors, respectively.

The inhibition efficiency of the inhibitor has been found out from the charge transfer resistance values using the Eq. (3) [59, 60]:

$$IE (\%) = \frac{R_{ct(inh)} - R_{ct(0)}}{R_{ct(inh)}} \times 100 \quad (3)$$

Where R<sub>ct (0)</sub> and R<sub>ct (inh)</sub> are the charge transfer resistance values without and with inhibitors, respectively.

### 2.2.3. Scanning Electron Microscopy (SEM)

The mild steel specimens of dimensions, 1.15 cm diameter and 0.15 cm height were abraded with a series of emery papers (grades 220, 400, 800, 1200 and 2400) and then washed with distilled water and ethanol. After immersion in 0.5M H<sub>2</sub>SO<sub>4</sub> solution in the absence and the presence of optimum concentration of inhibitor (PTT) and 0.2% KI at 303K for 2h, the specimens were cleaned with double-distilled water, dried with a cold air blaster, and then the SEM images were recorded using ZEISS scanning electron microscope.

### 2.2.4. Computational Details

Theoretical calculations of the compound were carried out using Density Functional Theory (DFT) as implemented in the Gaussian 09 quantum chemistry program. Geometry optimization was started from the X-Ray Diffraction (XRD) experimental atomic coordinates. Initial calculations were performed using the restricted B3LYP exchange and correlation functional and the B3LYP/6-311++G(d,p) basis set for all atoms, Default SCF and geometry convergence criteria were used and no symmetry constraints were imposed, harmonic frequency analysis based on analytical second derivate was used to characterize the optimized geometry as global minimum on the potential energy surface of the title molecule [61-66]. Geometry optimization of the molecule was done at B3LYP/6-311++G(d,p) level of theory then a Single point at the same theory level was performed for the calculations of the molecular orbital energies and dipole moments. The purpose of this work was to investigate whether there is a clear relationship between experimentally determined inhibition efficiency and quantum chemical data for the inhibitors studied. Quantum chemical parameters most relevant to their potential action as corrosion inhibitors such as E<sub>HOMO</sub> (highest occupied molecular orbital energy), E<sub>LUMO</sub> (lowest unoccupied molecular orbital energy), energy gap (ΔE), dipole moment (μ), ionization potential (I), electron affinity (A), chemical potential (π), absolute electronegativity (χ), global hardness (η), softness (σ), fraction of electrons transferred (ΔN), electrophilicity index (ω) and such electronic data as Mulliken atomic populations have been calculated and discussed. The ionization potential (I) and the electron affinity (A) are defined as follows deduced from Koopmans' theory [67, 68]:

$$I = - E_{HOMO} \dots \dots \dots (4)$$

$$A = - E_{LUMO} \dots \dots \dots (5)$$

Then the electronegativity and the global hardness were evaluated, based on the finite difference approximation, as linear combinations of the calculated I and A [61, 69]:

$$\chi = \frac{I+A}{2} \dots\dots\dots (6)$$

$$\eta = \frac{I-A}{2} \dots\dots\dots (7)$$

Softness is the inverse of hardness:

$$\sigma = \frac{1}{\eta} \dots\dots\dots (8)$$

The obtained values of  $\chi$  and  $\eta$  are used to calculate the fraction of the electron transferred,  $\Delta N$ , this parameter evaluates the electronic flow in a reaction of two systems with different electronegativities, in particular case; a metallic surface (Fe) and an inhibitor molecule.  $\Delta N$  is given as follows:

$$\Delta N = \frac{\chi_{Fe} - \chi_{inh}}{2(\eta_{Fe} + \eta_{inh})} \dots\dots\dots (9)$$

Where  $\chi_{Fe}$  and  $\chi_{inh}$  represent the absolute electronegativity of iron atom (Fe) and the inhibitor molecule, respectively;  $\eta_{Fe}$  and  $\eta_{inh}$  represent the absolute hardness of Fe atom and the inhibitor molecules, respectively. In order to calculate the fraction of electrons transferred, a theoretical value for the electronegativity of iron was employed  $\chi_{Fe} = 7$  eV and a global hardness of  $\eta_{Fe} = 0$  eV, by assuming that for a metallic bulk  $I = A$  because they are softer than the neutral metallic atoms [61, 62, 67, 70-72].

Recently, a new global chemical reactivity parameter has been introduced and known as electrophilicity index ( $\omega$ ). It is defined as [66, 67, 70, 71]:

$$\omega = \frac{\chi^2}{2\eta} \dots\dots\dots (10)$$

### 3. Results and Discussions

#### 3.1. Electrochemical Impedance Spectroscopy (EIS)

Impedance diagrams obtained for frequencies ranging from 100 kHz to 10 mHz at open circuit potential for mild steel in 0.5M H<sub>2</sub>SO<sub>4</sub> in the presence of various concentrations of PTT are shown in Fig. 2. All the plots display a single capacitive loop and they are not perfect semicircles. The difference has been attributed to frequency dispersion [73].

The fact that impedance diagrams have a semicircular appearance shows that the corrosion of steel is controlled by a charge transfer process and the presence of inhibitor does not alter the mechanism of dissolution of steel in H<sub>2</sub>SO<sub>4</sub> [74-76]. Fig. 2 reveals that increase in concentration of PTT results in increase in size of the semicircle, which is an indication of the inhibition of the corrosion process.

The equivalent circuit diagram is suggested as in Fig. 3, where, R<sub>s</sub> represents the solution resistance, R<sub>ct</sub> the charge transfer resistance, and CPE, the constant phase element. In most times, CPE is required for modeling the frequency dispersion behavior corresponding to different physical phenomena such as surface heterogeneity which results from surface roughness, impurities, dislocations, distribution of the active sites, adsorption of inhibitor and

formation of porous layers [77]. The impedance of CPE is given by the Eq. (11) [78]:

$$Z_{CPE} = Y_0^{-1} (j\omega)^{-\alpha} \dots\dots\dots (11)$$

Where Y<sub>0</sub> is proportionality coefficient,  $\omega$  is the angular frequency ( $\omega = 2\pi f$ ) and j is the imaginary number,  $\alpha$  is a measure of surface irregularity. Depending on the value of the exponent  $\alpha$ , Y<sub>0</sub> may be a resistance, R ( $\alpha = 0$ ); a capacitance, C ( $\alpha = 1$ ); Warburg impedance, W ( $\alpha = 0.5$ ) or an inductance, L ( $\alpha = -1$ ). According to Xiaojuan Wu et al. [79], the value of double layer capacitance, C<sub>dl</sub>, can be calculated for a parallel circuit composed of a CPE (Y<sub>0</sub>) and a resistor (R<sub>ct</sub>) using the Eq. (12) [78]:

$$C_{dl} = (Y_0 R_{ct}^{(1-\alpha)})^{1/\alpha} \dots\dots\dots (12)$$

The values of the charge transfer resistance, R<sub>ct</sub> double layer capacitance C<sub>dl</sub> and inhibition efficiency obtained from the above plots are given in Table 1. The impedance data listed in Table 1 indicate that the values of both R<sub>ct</sub> and IE (%) are found to increase by increasing the inhibitor concentration, while the values of C<sub>dl</sub> are found to decrease. This behavior was the result of an increase in the surface coverage by the inhibitor molecules, which led to an increase in the inhibition efficiency. The decrease in C<sub>dl</sub> values may be considered in terms of Helmholtz model [80]:

$$C_{dl} = \frac{\epsilon_0 \epsilon}{d} A \dots\dots\dots (13)$$

Where  $\epsilon_0$  is the permittivity of air,  $\epsilon$  the local dielectric constant, d the thickness of the film and A is the surface area of the electrode.

In fact, the decrease in C<sub>dl</sub> values can result from a decrease in local dielectric constant and/or an increase in the thickness of the electrical double layer. It could be assumed that the decrease of C<sub>dl</sub> values is caused by the gradual replacement of water molecules and other ions that were originally adsorbed on the electrode surface by adsorption of inhibitor molecules to form a protective film, which decreases the extent of the metal dissolution [81]. With higher concentration of PTT, either the thickness of the protective layer or the surface coverage by PTT increased due to more PTT electrostatically adsorbed on the electrode surface [82].

Nyquist plots for mild steel in 0.5M H<sub>2</sub>SO<sub>4</sub> in the presence of different concentrations of PTT in combination with 0.2% KI are shown in Fig. 4. The high-frequency part of the impedance and phase angles describes the behavior of an inhomogeneous surface layer, while the low-frequency contribution shows the kinetic response for the charge transfer reaction [83].

The impedance spectra, in this case, were fitted by a simple Randles circuit. Table 2 gives the values of the charge transfer resistance R<sub>ct</sub> obtained from above plots. It is found that the addition of KI further enhances R<sub>ct</sub> values and reduces C<sub>dl</sub> values. This can be attributed to the enhanced adsorption of PTT in the presence of KI because of the synergistic effect of iodide ions [84].

The inhibitive effect of iodide ions is often attributed to its adsorption on the metal surface which depends on its large ionic radius and high hydrophobicity [85]. On the other hand, the exponential term of the CPE between 0.8 and 0.9 indicate that there is no diffusion process normally evidenced by an exponential term of ca. 0.5 [83].

### 3.2. Polarization Measurements

Potentiodynamic anodic and cathodic polarization scans were carried out at 303 K in 0.5M H<sub>2</sub>SO<sub>4</sub> solution with different concentrations of PTT and 0.2% KI. Fig. 5 shows anodic and cathodic polarization curves of mild steel in 0.5M H<sub>2</sub>SO<sub>4</sub> blank solution and in the presence of different concentrations (0.1–0.5 mM) of PTT. The linear Tafel segments of the cathodic and anodic curves were extrapolated to the point of intersection to obtain the corrosion potential ( $E_{\text{corr}}$ ) and corrosion current density ( $I_{\text{corr}}$ ). The electrochemical parameters determined from polarization curve are summarized in Table 3.

It is seen that PTT inhibitor shifts both the cathodic and anodic branches of the polarization curves of the pure acid solution to lower values of current density indicating the inhibition of both the hydrogen evolution and mild steel dissolution reactions. According to Ferreira et al. [86], if the displacement  $E_{\text{corr}} > 85$  mV, the inhibitor acts as a cathodic or anodic inhibitor, if the displacement  $E_{\text{corr}} < 85$  mV, the inhibitor is considered as mixed type inhibitor [87]. In the present study, in Table 3, the maximum shifting in the  $E_{\text{corr}}$  value compared to the blank is 90 mV for PTT alone, indicating that the inhibitor studied are a cathodic inhibitor. Some retardation of the anodic reaction is observed but cathodic polarization is clearly dominant. PTT inhibited the hydrogen evolution more than anodic dissolution of mild steel. It can also be seen that PTT decreases the corrosion current densities at all the studied concentrations, meaning that the corrosion rate of steel is reduced significantly.

The addition of KI further reduces the  $I_{\text{corr}}$  values. Values of inhibition efficiency are found to increase with increase in the concentration of PTT reaching maximum value 91.6% at 0.5 mM and the addition of KI improved the inhibition efficiency of PTT to 97.7%. Moreover, the anodic and cathodic Tafel slope values are different from the ones obtained with and without the presence of PTT, respectively, suggesting that the mechanism of the reaction of mild steel in 0.5M H<sub>2</sub>SO<sub>4</sub> is influenced by the presence of PTT. The addition of KI affects slightly the values of  $\beta_c$  and  $\beta_a$ . The maximum shifting in the  $E_{\text{corr}}$  value in the presence of 0.2% KI is 35 mV. The values of corrosion potential indicate that a mixed-type control and PTT is an inhibitor of mixed-type with predominant effect on the cathodic reaction for the corrosion of mild steel in 0.5M H<sub>2</sub>SO<sub>4</sub>. The inhibition efficiency obtained from polarization measurement is in good agreement with results obtained from EIS tests.

### 3.3. Weight Loss Measurements

Values of the inhibition efficiency obtained from the weight loss measurements of mild steel for different concentrations of PTT in 0.5M H<sub>2</sub>SO<sub>4</sub> at 303 K in the absence and the presence of 0.2% KI after 1 h of immersion [1-9]. PTT inhibit the corrosion of mild steel in 0.5M H<sub>2</sub>SO<sub>4</sub> solution at all concentrations used in this study and the corrosion rates (CR) is seen to decrease continuously with increasing additive concentration at 303K. Indeed, corrosion rate values of mild steel decrease when the inhibitor concentration increases while IE (%) values of PTT increase with the increase of the concentration, the maximum IE (%) of 91.62% is achieved at 0.5 mM [58, 59]. The inhibition of corrosion of mild steel by PTT can be explained in terms of its adsorption on the metal surface. This compound can be adsorbed on the metal surface by the interaction between lone pairs of electrons of nitrogen and sulfur atoms of the inhibitor and the metal surface. This process is facilitated by the presence of vacant orbitals of low energy in iron atom, as observed in the transition group metals [88-90].

Moreover, the formation of positively charged protonated species in acidic solutions facilitates the adsorption of the compound on the metal surface through electrostatic interactions between the organic molecules and the metal surface.

On the other hand, it can be seen from Table 4 that the addition of KI in the solution improved the inhibition efficiency of PTT significantly. The synergistic effect between PTT and KI can be due to coulombic interactions between chemisorbed I<sup>-</sup> and organic polycations PTT<sup>+</sup>. The stabilization of adsorbed PTT<sup>+</sup> on the iron surface which may be caused by electrostatic interactions with I<sup>-</sup> ions leads to more surface coverage and consequently greater corrosion inhibition.

### 3.4. Effect of Immersion Time on Corrosion of Mild Steel

In order to assess the stability of inhibitive behavior of inhibitor on a time scale, weight loss measurements were performed in 0.5M H<sub>2</sub>SO<sub>4</sub> in absence and presence 0.5 mM of PTT and 0.2% KI for different immersion time at temperature 303 K. The table 5 gives the obtained results.

This table shows that the inhibition efficiency of PTT in absence and presence KI decreased with immersion time. Shriver et al. [91-93] and Ishtiaque et al. [94] explained that decrease in inhibition for long period of immersion can be attributed to the depletion of available inhibitor molecules in the solution due to chelate formation between iron and the inhibitor ligands.

### 3.5. Synergism Parameters

Halides ions have been widely reported to synergistically increase the inhibition of the corrosion of metals in acidic medium by organic compounds [95-106]. The enhanced corrosion inhibition on addition of the halides was attributed to promotion of the adsorption of the organic

molecules on the metal surface. The effect of KI on the inhibition efficiency of PTT inhibitor was investigated by EIS measurements in the present work at 303 K. Table 6 gives values of the inhibition efficiency for the corrosion of mild steel in 0.5M H<sub>2</sub>SO<sub>4</sub> in the presence of 0.5 mM PTT at 303K and different concentrations of KI. It can be seen that the maximum synergistic effect is obtained for a KI concentration of 0.2%. Fig. 6 shows the plot of different values of R<sub>ct</sub> for all concentrations of PTT inhibitor in the absence and presence of 0.2% KI at 303 K after one hour of immersion. Fig. 6 reveals clearly the existence of synergism phenomenon between iodide ions and PTT molecules considering that R<sub>ct</sub> was increased on addition of the iodide ions to PTT inhibitor in comparison to PTT alone.

To further confirm whether synergism is taking place, one has to determine the synergism parameter (S), the synergism parameters were calculated using the relationship proposed by Aramaki and Hackerman [97, 102]:

$$S = \frac{1 - IE_{1+2}}{1 - IE'_{1+2}} \dots\dots\dots (14)$$

Where, IE<sub>1+2</sub> = (IE<sub>1</sub> + IE<sub>2</sub>) - (IE<sub>1</sub> × IE<sub>2</sub>); IE<sub>1</sub> is the inhibition efficiency (no exprimed in percent) of substance 1 (PTT), IE<sub>2</sub> is the inhibition efficiency of substance 2 (KI), IE' <sub>1+2</sub> is the measured inhibition efficiency for substance 2 in combination with substance 1. S approaches 1 when no interaction between the inhibitor compounds exists, while S>1 points to a synergistic effect. In the case of S<1, the adsorption of each compound antagonizes the others adsorption [102, 107]. Values of S are given in Table 7.

It can be seen from this table that most of values are greater than unity; except for the lower concentration. This result indicates that the increase in inhibitor efficiency is generated by the addition of KI to PTT due to a synergistic effect and this may be related to adsorption of iodide ions on metal surface that caused the increase of adsorption of inhibitor. In addition, the synergistic effect is more pronounced for the optimal concentration. However, a careful inspection of this table suggests that a competitive adsorption appears for the lower concentration of PTT [108].

Globally, the inhibition efficiency measured for different methods was estimated at about 91.6% in the absence of 0.2% KI and 97% in the presence of KI, the inhibition efficiency obtained from weight loss and electrochemical measurements are in good agreement (Fig. 7).

**3.6. Effect of Temperature**

In order to study the effect of temperature on the inhibition characteristic of triazole derivative (PTT), weight loss measurements were performed at different temperatures from 298 to 323 K in the absence and presence of different additives for 1 h immersion time. The results are given in Table 8.

It can be seen that, the inhibition efficiencies of PTT decrease with increase in the temperature in the absence and presence of 0.2% KI. However, these values decrease more rapidly (around 15 %) with temperature in the case of PTT alone, which indicated desorption of inhibitor molecules to some extent with increasing temperature [1]. The activation energy (E<sub>a</sub>) for the corrosion process in the absence and presence of PTT was evaluated from Arrhenius equation [59, 78, 109]:

$$\text{Log CR} = -\frac{E_a}{2.303 RT} + \text{log A} \dots\dots\dots (15)$$

Where CR is the corrosion rate, E<sub>a</sub> is the apparent activation energy, A the pre-exponential factor, R the universal gas constant (8.314 J K<sup>-1</sup>mol<sup>-1</sup>), T the absolute temperature. The Arrhenius plots for mild steel immersed in 0.5 M H<sub>2</sub>SO<sub>4</sub> are shown in Fig. 8 for a blank solution and in the presence of PTT and (PTT + KI). Straight lines are obtained. The values of E<sub>a</sub> obtained from the slopes of the lines (-E<sub>a</sub>/2.303R) are listed in Table 9.

It is evident that the value of E<sub>a</sub> is higher for inhibited solution than that for uninhibited solution and the value of E<sub>a</sub> for the mixture (PTT + KI) is the highest one. The increase in E<sub>a</sub> values confirms stronger physisorption of the inhibitor on the mild steel surface, which is facilitated by the presence of KI. Physisorption is small but important because it is the preceding stage of chemisorption. The triazole molecules create a barrier to charge and mass transfer. The increase in E<sub>a</sub> values might also be correlated with the increased thickness of double layer [110]. To calculate enthalpy and entropy of activation for corrosion process transition state the Eq. (16) was used [59, 78, 111]:

$$\text{CR} = \frac{RT}{Nh} \exp\left(\frac{\Delta S^*}{R}\right) \exp\left(-\frac{\Delta H^*}{RT}\right) \dots\dots\dots (16)$$

Where h is the Planck's constant, N is the Avogadro's number, ΔS\* is the entropy of activation and ΔH\* is the enthalpy of activation. Fig. 8b, showed the plot of log (CR/T) against 1/T. The plots obtained are straight lines and the values of ΔH\* are calculated from their gradient (ΔH\* = - slope\*2.303R) and ΔS\* from intercept [log (R/Nh) + ΔS\*/2.303R]. The calculated data listed in Table 9.

The positive signs of ΔH\* reflect the endothermic nature of mild steel dissolution process in the presence of PTT. The value of ΔS\* is higher for inhibited solution than that for the uninhibited solution, suggesting an increase in randomness on going from reactants to the activated complex. The increase in values of entropy by the adsorption of PTT molecules on metal surface from the acid solution could be regarded as quasi-substitution between the inhibitor in the aqueous phase and H<sub>2</sub>O molecules on electrode surface. In such condition, the adsorption of PTT molecules was followed by desorption of H<sub>2</sub>O molecules

from the electrode surface. Thus increase in entropy of activation is attributed to solvent (H<sub>2</sub>O) entropy [86, 112]. In the case of the mixture (PTT + KI) the value of  $\Delta S^*$  is the highest one. This can be attributed to the gradual replacement of water molecules by the iodide ions and by the adsorption of the PTT molecules on the metal surface, decreasing the extent of dissolution reaction.

### 3.7. Adsorption Isotherm

Basic information on the interaction between the inhibitor and the mild steel surface is obtained from various isotherms. Adsorption of this organic inhibitor has displaced the water molecules from the metal surface. The most commonly used adsorption isotherms are Langmuir, Temkin, and Frumkin. Langmuir adsorption isotherm was found to be best fit. The degree of surface coverage ( $\theta$ ) for different concentrations of inhibitor in 0.5 M H<sub>2</sub>SO<sub>4</sub> solution has been evaluated by the polarization measurements. According to the Langmuir adsorption isotherm, the surface coverage ( $\theta$ ) is related to the inhibition concentration  $C_{inh}$  by the Eq. (17) [59, 60]:

$$\frac{C_{inh}}{\theta} = \frac{1}{K_{ads}} + C_{inh} \dots\dots\dots (17)$$

Where  $C_{inh}$  is the inhibitor concentration and  $K_{ads}$  is the equilibrium constant for adsorption-desorption process.

The plots of  $C_{inh}/\theta$  versus  $C_{inh}$  (Fig. 9) gives straight lines for all temperatures with a slope of unity is observed and the linear correlation coefficient is 0.999 which suggests that the adsorption obeys Langmuir adsorption isotherm. The adsorption of PTT inhibitor on the metal surface can occur on the basis of donor-acceptor interactions between the  $\pi$ -electrons of the heterocyclic compound and the lone pairs of the hetero-atoms and vacant d-orbitals of iron surface atoms [113-115]. From the intercept,  $K_{ads}$  is calculated, and by using its values, the values of  $\Delta G_{ads}^0$  were calculated by the Eq. (18) [59, 60]:

$$\Delta G_{ads}^0 = -RT \ln (55.5 K_{ads}) \dots\dots\dots (18)$$

Where  $K_{ads}$  is the adsorptive equilibrium constant,  $\Delta G_{ads}^0$  is the free energy of adsorption, R is the gas constant and T is the absolute temperature. The value of 55.5 is the molar concentration of water in solution in mol. L<sup>-1</sup> [116].

The addition of KI did not change the adsorption behavior of PTT. It can be concluded that the inhibition actions of (PTT+ KI) are mainly attributed to the adsorption of PTT. The PTT molecules may have stronger adsorption abilities than iodide ions, as indicated by their inhibition efficiencies.

On the other hand, the values of the free energy of adsorption as calculated from the Eq. (18) in the absence and the presence of KI are -36.2 and -38.1 kJ.mol<sup>-1</sup>, respectively. The largest negative values of  $\Delta G_{ads}^0$  ensure the spontaneity of the adsorption process and stability of the adsorbed layer on the steel surface and also indicate that PTT is strongly adsorbed on the mild steel surface and this adsorption is greater in the presence of KI [117]. Generally, values of  $\Delta G_{ads}^0$ , around -20 kJ.mol<sup>-1</sup> or lower are consistent

with the electrostatic interaction between the charged molecules and charge metal, such as physisorption. When it is around -40 kJ.mol<sup>-1</sup> or higher values it involve charge sharing or charge transfer from organic molecules to the metal surface to form a coordinate type of bond that is chemisorption [118, 119]. The calculated values range from -30 to -40 kJ.mol<sup>-1</sup>. This indicates that PTT is adsorbed chemically and physically on steel surface in 0.5M H<sub>2</sub>SO<sub>4</sub> solution. The unshared electron pairs of heteroatom interact with d-orbital of iron atom of steel to provide a protective chemisorbed film [120].

PTT may adsorbed on a metal surface in the form of a neutral molecule via the chemisorption mechanism [88] involving the sharing of electrons between the nitrogen, sulphur atom and iron. The second mode (physisorption) is possible if one examines also the activation energy ( $E_a$ ) that increases in the presence of PTT. Adsorption of PTT can also occur through  $\pi$  electron interactions between the triazole group structure of molecules and the metal surface. Therefore, we may suggest that the adsorption may occur through the lone pairs of heteroatoms and  $\pi$  electrons of the PTT molecules which outweigh the adsorption due to the cationic form of the PTT molecule on the metal surface. We can conclude that adsorption acts simultaneously by chemisorption and physical adsorption [121].

### 3.8. Scanning Electron Microscopy (SEM)

Fig. 10 represents the SEM images of mild steel samples under various conditions studied in this work. Fig. 10(a) is the image of newly polished sample before placing in 0.5 M H<sub>2</sub>SO<sub>4</sub>. Fig. 10(b) shows the same sample after immersing in the blank solution for 2h at 303 K. The appearance of corrosion products is clearly observed. Fig. 10(c) was taken from a sample in acid solution containing PTT alone and finally Fig. 10(d) represents the metal sample after immersing in solution containing both PTT (0.5 mM) and potassium iodide (0.2%). It can be seen from Fig. 10(b) that the mild steel surface was strongly damaged with deep cavities in the absence of the inhibitor due to metal dissolution in corrosive solution. The image of steel surface exposed to PTT containing solution (Fig. 10c) exhibits good surface and no damage, the sample has smooth surface compared with that of the sample immersed in 0.5 M H<sub>2</sub>SO<sub>4</sub> with few small notches. No damages expect polishing lines are observed in the micrograph after the addition of iodide ions to the corrosive solution (Fig. 10d). The steel surface in the presence of KI + PTT mixture (Fig. 10d) is the smoothest surface and thus the mixture is a more effective inhibitor. The resemblance of the Fig. 10(d) to that of (a) is appreciable and proves the excellent corrosion prevention of PTT and iodide ions combined. The later effect is due to synergistic interactions between PTT and iodide ions resulting in higher inhibition efficiency. This indicates that the combination of PTT and KI hinders the dissolution of

iron and thereby reduces the rate of corrosion, and it reveals good protection against corrosion.

### 3.9. DFT Calculations

The inhibitory effect of the inhibitors regularly depends on the adsorption of these molecules on the metal surface, this adsorption depending on the molecular structures. Several quantum chemical methods and molecular modeling techniques are very often used in corrosion inhibition studies in order to ascertain the relationship between corrosion inhibition efficiency and molecular properties, and consequently, to estimate the trends in the binding energy between inhibitors chemisorbed and/or physisorbed on metal surfaces [52, 61, 62, 66, 122, 123]. To investigate the relationship between the molecular structure of this triazole derivative (PTT) and its inhibition effect, quantum chemical calculations were performed. DFT is a very powerful technique to probe the inhibitor/surface interaction and to analyze experimental data. DFT methods have become very popular in the last decade due to their accuracy that is similar to other methods in less time and with a smaller investment from the computational point of view [124]. The optimized structures of the triazole derivative in the neutral form including their HOMO and LUMO distributions density at the B3LYP/6-31G(d,p) level are presented in Fig. 11, the graphics was done thanks to GABEDIT. Positive and negative phase is represented in red and blue color, respectively.

Quantum chemical parameters such as:  $E_{\text{HOMO}}$ ,  $E_{\text{LUMO}}$ ,  $\Delta E$ ,  $\mu$ ,  $\chi$ ,  $\eta$ ,  $\sigma$ ,  $\omega$  and  $\Delta N$  affect the inhibitory effectiveness [71]. These quantum chemical characteristics for the estimated structure are calculated from equations 4 to 10 and presented in Table 10. The frontier molecular orbitals play an important role in the electric and optical properties [125]. The HOMO represents the ability to donate an electron, LUMO as an electron acceptor. Inspection of Table 10 reveals that the calculated HOMO and LUMO energies are, respectively, -7.731, -0.260, the gap is 7.471. The negative values of  $E_{\text{HOMO}}$  indicate that adsorption of this inhibitor on the steel surface is important [70]. Generally, the higher values of  $E_{\text{HOMO}}$  indicate an increase for the electron donor and this means a better inhibitory activity with increasing adsorption of the inhibitor on a metal surface, whereas  $E_{\text{LUMO}}$  indicates the ability to accept electron of the molecule and strong electronic interactions between inhibitor and metal surface, this later is -0.260 eV indicates the easiness for this molecule to receipt electrons from the d orbital of the metal. The adsorption ability of the inhibitor to the metal surface increases with increasing of  $E_{\text{HOMO}}$  and decreasing of  $E_{\text{LUMO}}$ . Therefore high  $E_{\text{LUMO}}$  and low  $E_{\text{LUMO}}$  values are associated with high electron donating ability of inhibitor and thereby increasing the corrosion Inhibition efficiency [126, 127]. Large values of the energy gap ( $\Delta E$ ) imply high electronic stability and then low reactivity; whereas low values imply that it will be easier to

remove an electron from the HOMO to the LUMO, which can result in highly efficient inhibition. These results showed that the mechanism of inhibition is based primarily on an adsorption process performed by charge transfer from the inhibitor to the metal [70]. Furthermore, less negative HOMO energy and the smaller energy gap ( $\Delta E_{\text{HOMO-LUMO}}$ ) are reflected in a stronger chemisorption bond and perhaps greater inhibition efficiency [90, 128]. This can be possible because removing electrons from HOMO needs a small energy. This confirms the obtained results and it is in a good agreement with the values of  $\Delta N$  [129]. Low values of the energy gap ( $\Delta E$ ) will provide good inhibition efficiencies because the excitation energy to remove an electron from the last occupied orbital will be low. A molecule with a low energy gap is more polarizable and is generally associated with a high chemical reactivity. The calculation in Table 10 shows that PTT has smaller energy gap value indicating that PTT can easily adsorb on the metal surface causing higher protection. According to literature, there is a lack of agreement on the correlation between dipole moment and inhibition mechanism. The high value of dipole moment probably increases the adsorption between a chemical compound and metal surface [130]. Meanwhile, a survey of the literature reveals that several irregularities have appeared in the case of correlation of the dipole moment with inhibitor efficiency [131, 132]. However, increasing values of  $E_{\text{HOMO}}$  and  $\mu$  may facilitate adsorption by influencing the transport process through the adsorbed layer and lead to better inhibition efficiency [90]. From Table 10, the high compound polarity (dipole moment equal to 4.381 Debye) which is higher than the dipole moment  $\text{H}_2\text{O}$  (1.88 Debye). The high dipole moment value of this compound probably indicates strong dipole-dipole interactions between them and the metal surface and facilitates electrostatic interaction between the electric field, due to the metal charge and the electric moment of this inhibitor, and contributes to their better adsorption [133]. Therefore, a quasi-substitution process occurs between molecules of PTT and water ones on the steel area, with desorption of water molecules from the metal. Thus, the inhibition process can be done [134].

High ionization energy ( $I = 7.731$  eV) indicates high stability, the number of electrons transferred ( $\Delta N$ ) was also calculated and tabulated in Table 10. The fraction of electrons transferred ( $\Delta N$ ) values describes the inhibition achieved from electron donations. The values ( $\Delta N$ ) are correlated with the inhibition efficiency resulting from the electron donation. According to Lukovits [66], if ( $\Delta N$ ) < 3.6, the inhibitory efficiency is increased by increasing the ability inhibitor to give electrons to metal surface, while it decreased if  $\Delta N > 3.6$  (electron). It is apparent from Table 10 that  $\Delta N$  value is positive and is below 3.6, this means that the inhibitor (PTT) has the tendency to donate electrons to the metal surface by chemisorption process [62]. The inhibitory power is also influenced by the value of the

electrophilicity index ( $\omega$ ). The inhibitor effectiveness increases with the decrease of the  $\omega$  value. The value of  $\omega$  (2.137) agrees with the high value of the protection rate [134]. The electronegativity value of the inhibitor molecule is equal to 3.996. This electronegativity value ( $\chi=3.996$ ) being inferior to that of iron suggests an exchange of electron between the high occupied molecular orbital of the inhibitor (HOMO) and the unoccupied 3d orbitals of iron. This electron transfer is more probable than that from the occupied 4s orbital of Fe to the low unoccupied molecular orbital (LUMO) of the inhibitor [71]. Absolute hardness ( $\eta$ ), and softness ( $\sigma$ ), is important properties to measure the molecular stability and reactivity. It is apparent that the chemical hardness fundamentally signifies the resistance towards the deformation or polarization of the electron cloud of the atoms, ions or molecules under small perturbation of chemical reaction. A hard molecule has a large energy gap and a soft molecule has a small energy gap [135]. In our present study PTT with low hardness value +3.736 eV compared with other compound have a low energy gap. Normally, the inhibitor with the least value of global hardness (hence the highest value of global softness) is expected to have the highest inhibition efficiency. For the simplest transfer of electron, adsorption could occur at the part of the molecule where softness ( $\sigma$ ), which is a local property, has a highest value. PTT with the softness value of +0.268 eV has a highest inhibition efficiency [136].

The HOMO and LUMO electronic density distributions of PTT are plotted in Fig. 11. It can be observed that for the molecule of PTT, HOMO and LUMO are distributed around heteroatoms and aromatic rings, indicating that these heteroatoms and aromatic rings on which negative charge density is high, are main adsorption centers of the triazole derivative by the metal surface, by formation of donor-acceptor coordination bonds with vacant

"d" orbitals of the iron [124]. Thus, the bond with the metal from this active sites will be easily formed, rather than the others atoms. The inhibition efficiency of the compounds depends on many major factors, for example the number of adsorption active centres in the molecule and their charge density, molecule size, mode of adsorption, and formation of metallic complexes. The effect of substituents in the compounds on inhibition of corrosion of mild steel by PTT will be rationalized by use of global reactivity indexes, in the form of the Mulliken charges. Theoretical calculation of the charge density on the heteroatoms in the molecular structure of PTT reinforces the suggestion that the inhibitory effect results from the groups constituting the rigid centre of the molecule and their adsorption by the surface of the mild steel. This distribution thus ensures strong adsorption by the metal surface [70]. Mulliken charge analysis is used to estimate the adsorption centers of inhibitors, the results were presented on the atoms in the optimized structure (Fig.11). It is possible to observe that the heteroatoms afford a noticeable excess of negative charges could act as a nucleophilic reagent [62, 137]. The effective atomic charges from Mulliken populations presented in table 11 show that the highest negative charges were located on S (-0.484), N1 (-0.301) and N4 (-0.008) atoms as well as some carbon atoms of the aromatic rings C8 (-0.533), C10 (-0.311) and C11 (-0.595). These atoms are the more negative charge centers that could give electrons to the Fe atoms in order to coordinate it, and the positive charge centers that can accept electrons from 3d orbital of the Fe atoms to form feedback bond, thus further strengthening the interaction of inhibitor and Fe surface. This implies that PTT has potential heteroatoms that can be adsorbed in positive centers on the metallic surface through a donor-acceptor type reaction [138].

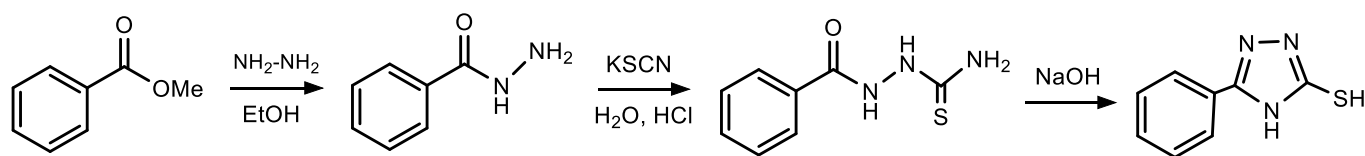


**Fig. 1:** Scheme of synthesis of 5-Phenyl-4H-1,2,4-triazole-3-thiol (PTT)

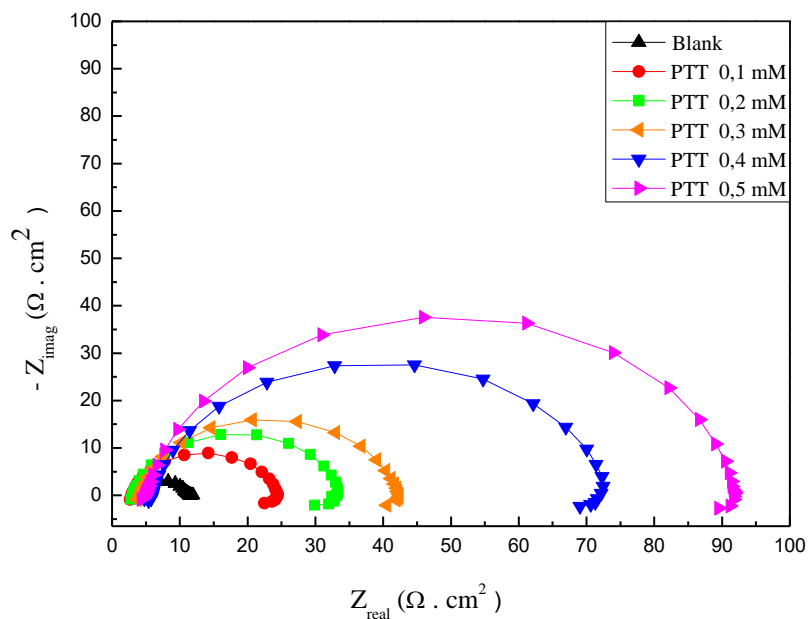


Fig. 2. Nyquist plots for mild steel in 0.5 M H<sub>2</sub>SO<sub>4</sub> containing different concentrations of PTT

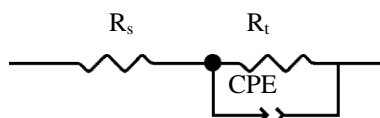


Fig. 3. The equivalent circuit of the impedance spectra obtained for PTT in 0.5M H<sub>2</sub>SO<sub>4</sub>

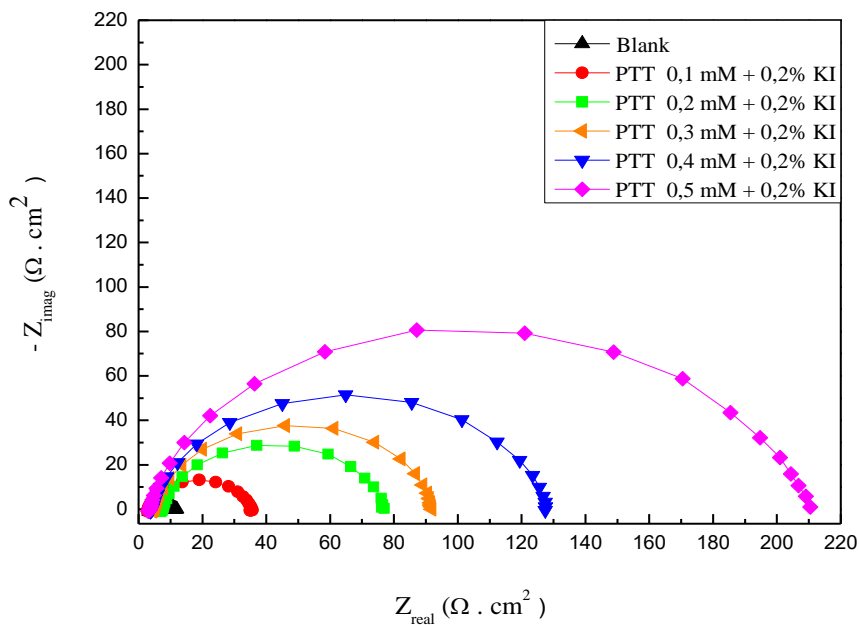
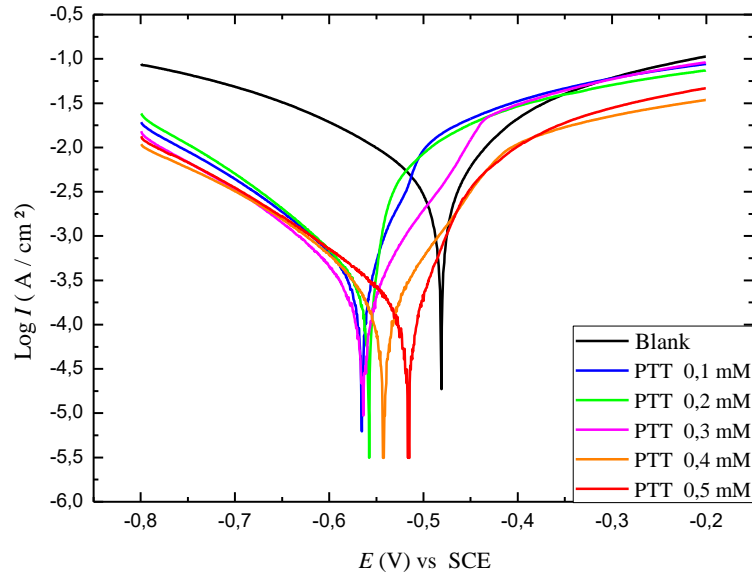
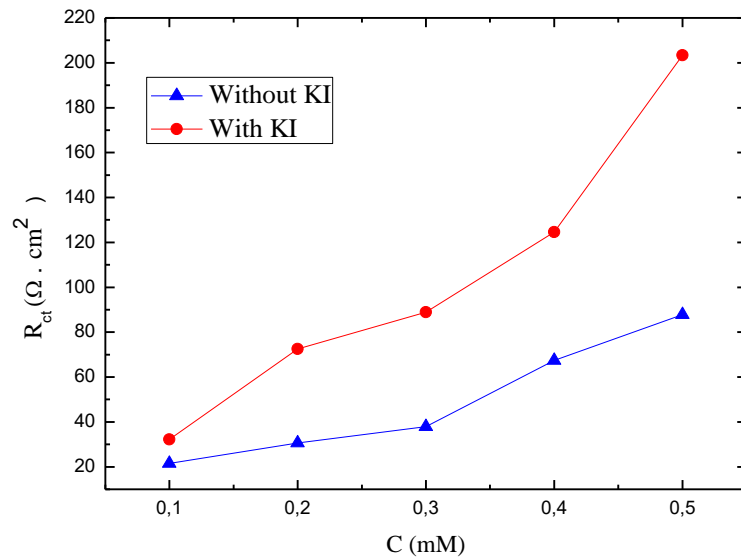


Fig. 4. Nyquist plots for mild steel in 0.5M H<sub>2</sub>SO<sub>4</sub> containing different concentrations of PTT in the presence of KI 0.2 %



**Fig. 5.** Potentiodynamic polarization curves of mild steel in 0.5M H<sub>2</sub>SO<sub>4</sub> for different concentrations of PTT at 303 K.



**Fig. 6.** R<sub>ct</sub> values in the absence and presence of 0.2% KI for different concentrations of PTT

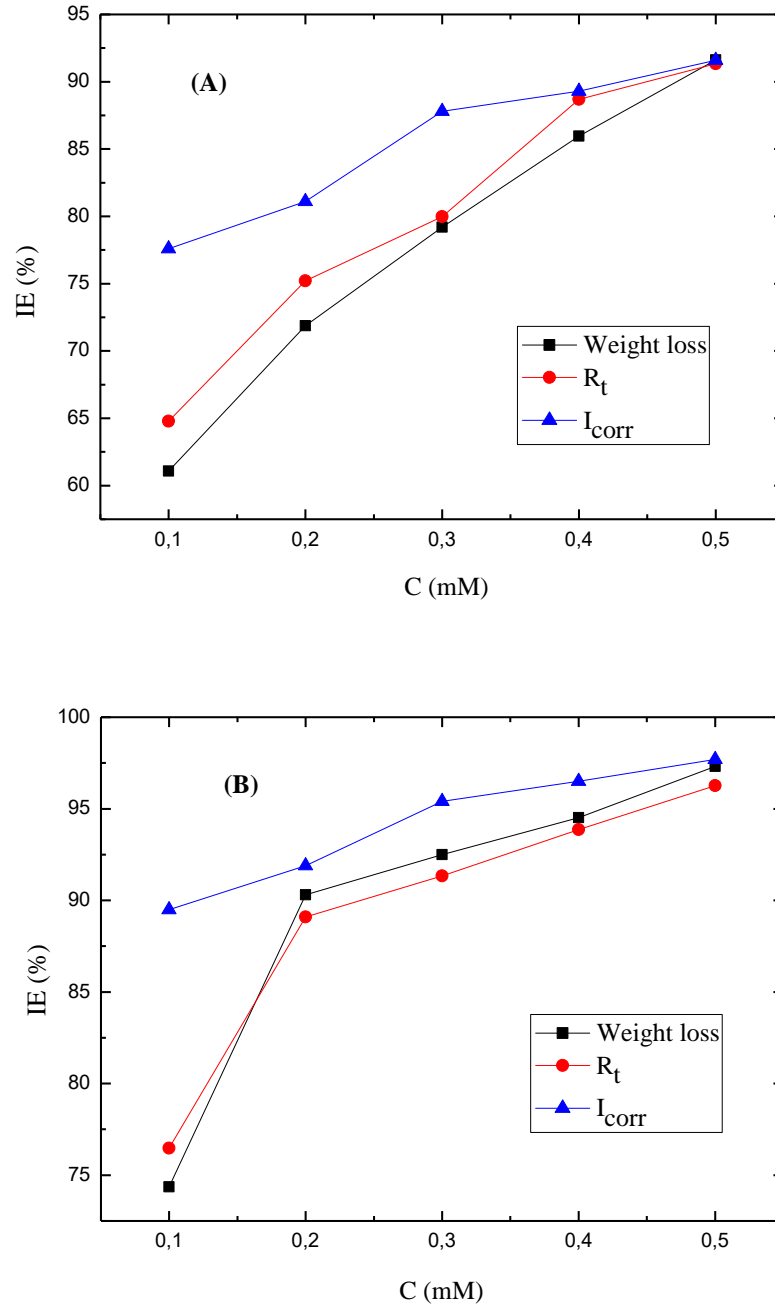


**Fig. 7.** Inhibition efficiency vs inhibitor concentrations calculated by different methods: (A) in the absence of 0.2% KI, (B) in the presence of 0.2% KI

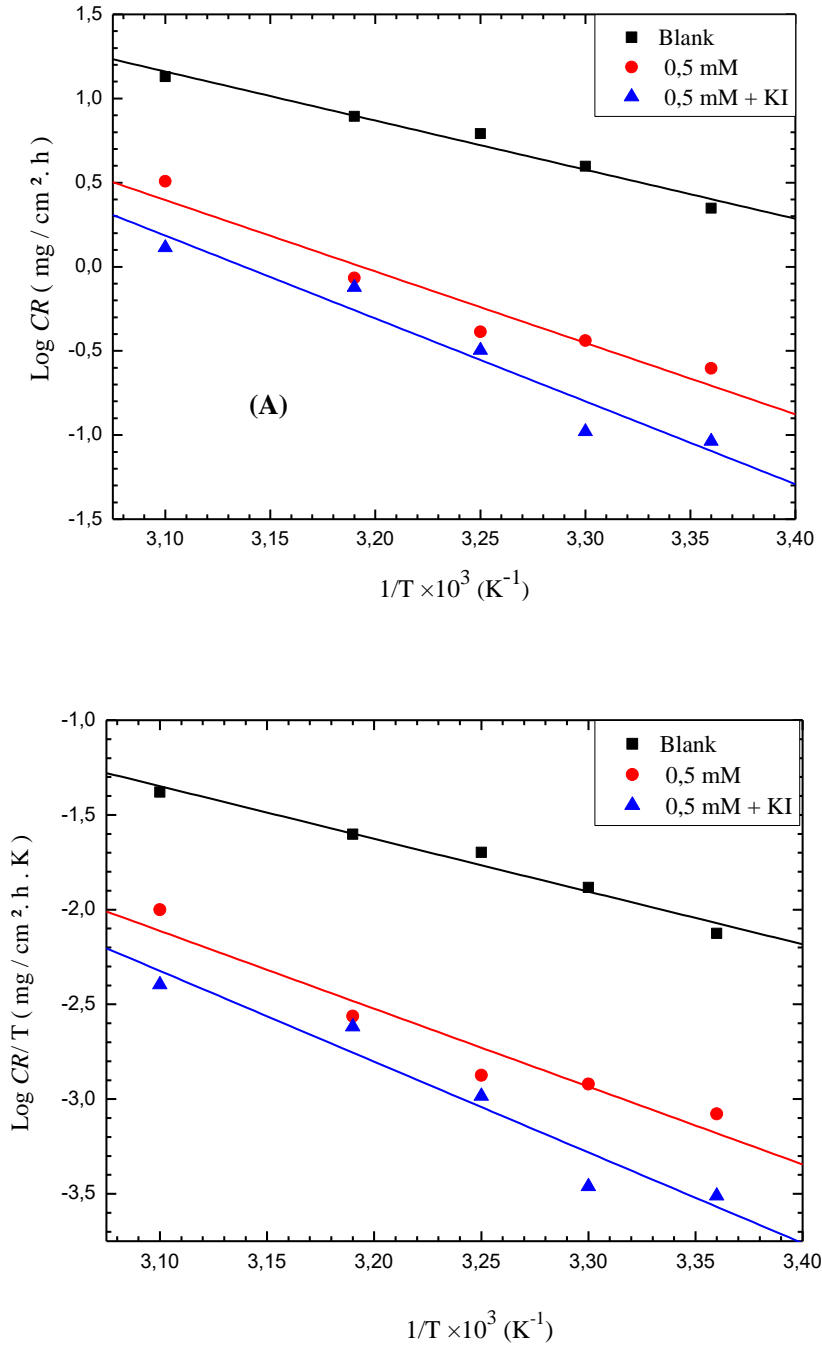


**Fig. 8.** Arrhenius plots of: (a) log CR vs. 1 / T; (b) log (CR / T) vs. 1 / T for the mild steel in 0.5 M H<sub>2</sub>SO<sub>4</sub> solution in the absence and presence of 0.5 mM PTT and 0.5 mM PTT + 0.2% KI

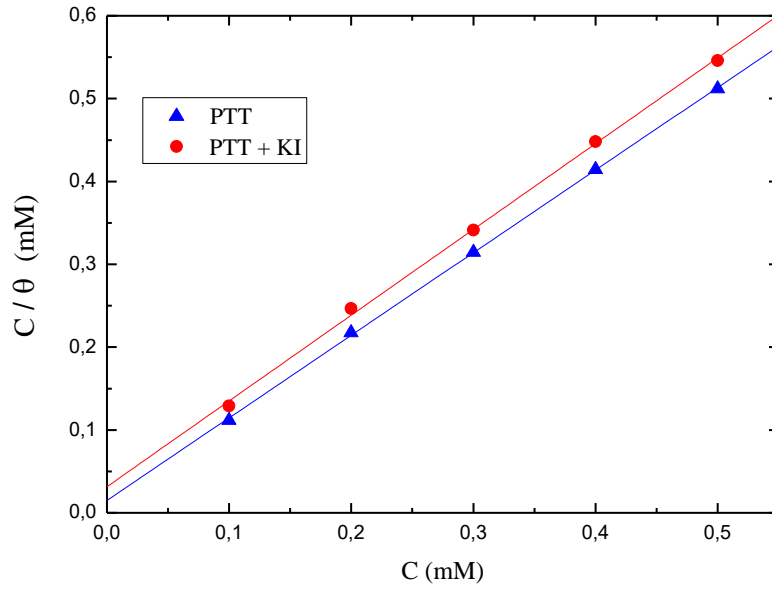


Fig. 9. Langmuir's adsorption isotherm of PTT and (PTT + KI) on the mild steel surface in 0.5M H<sub>2</sub>SO<sub>4</sub> from polarization measurements

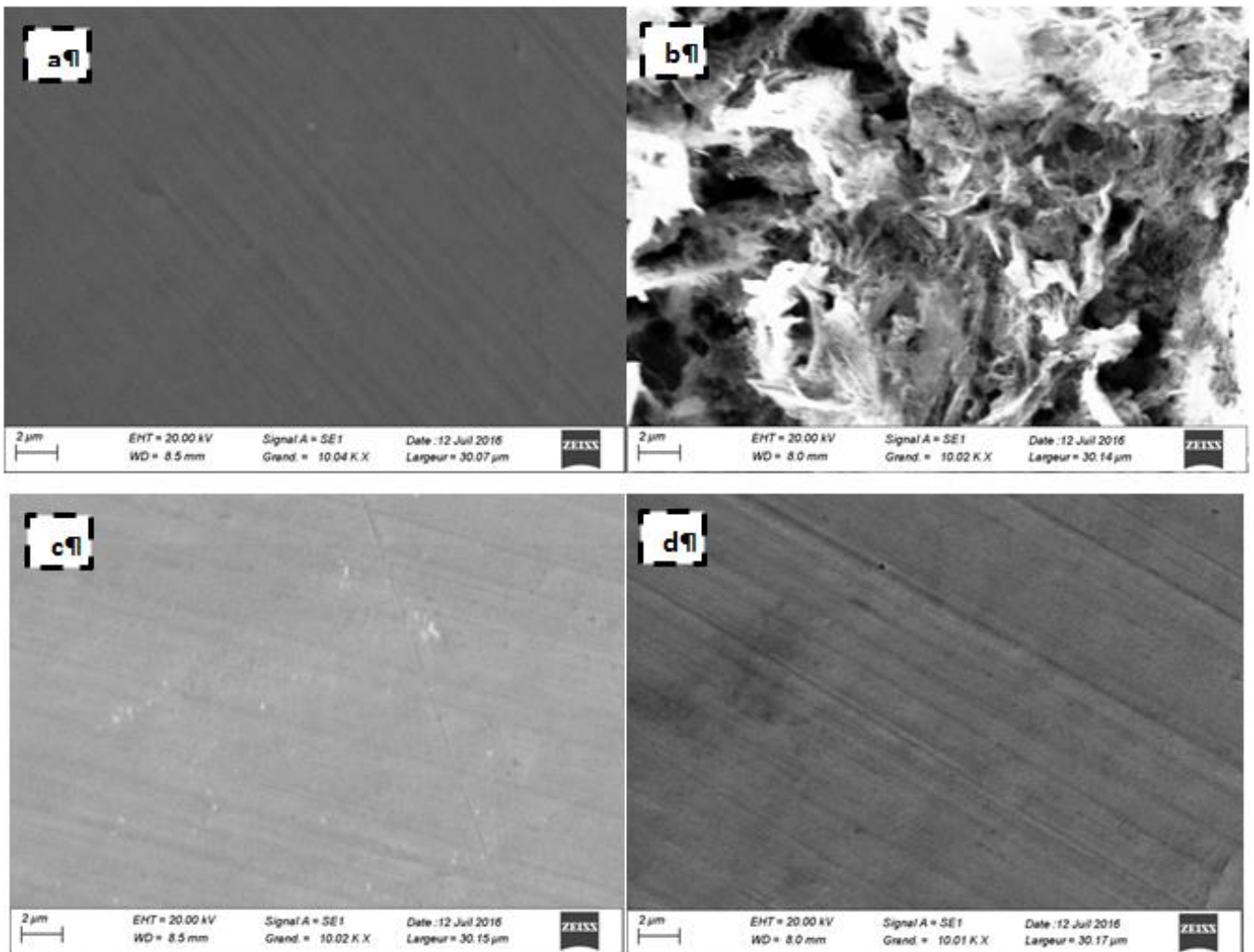
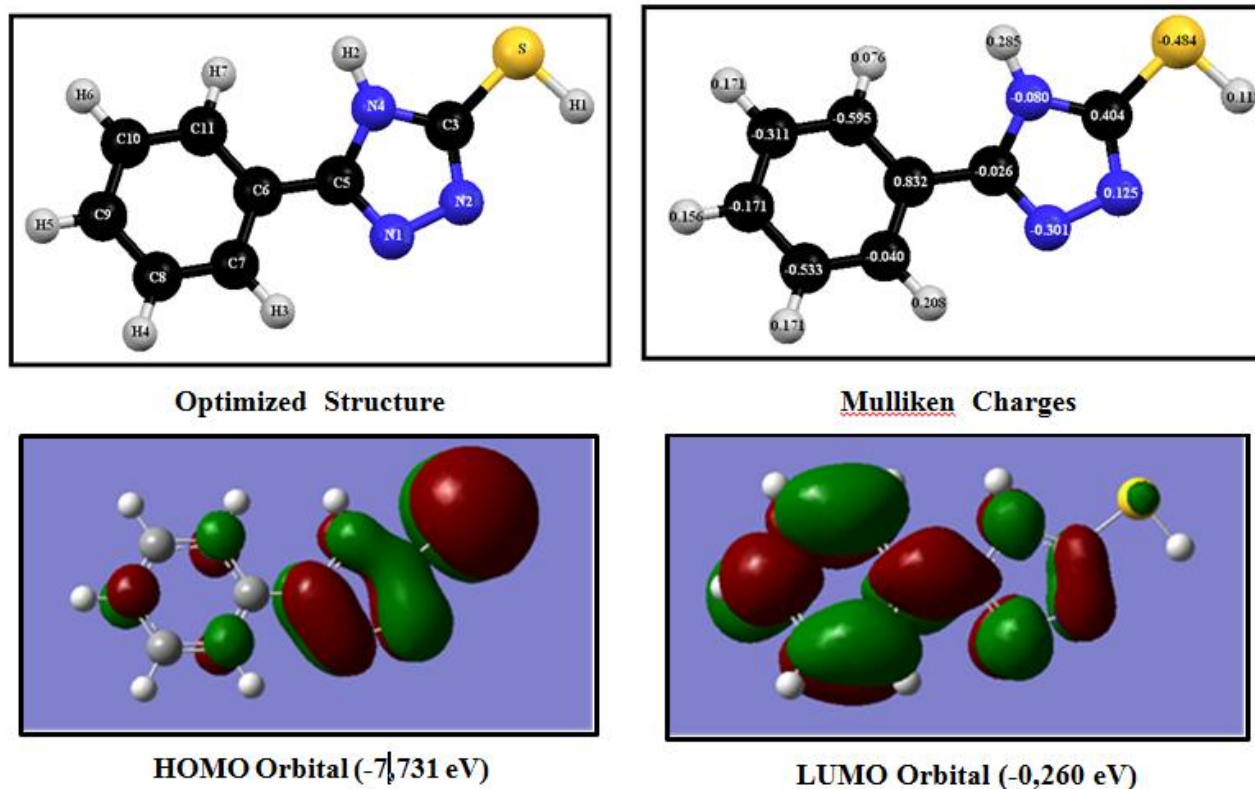


Fig. 10. SEM image of the surface of mild steel after immersion for 2 h in 0.5 M H<sub>2</sub>SO<sub>4</sub> solution at 303K: (a) Before immersion (polished) (b) After immersion without inhibitor (c) With inhibitor (PTT) (d) With inhibitor and in presence of KI



**Fig. 11.** Optimized structure, Mulliken charges density and Frontier molecule orbital density distributions: HOMO (left) and LUMO (right) of PTT given by the B3LYP/6-31(d,p)

**Table 1.** Electrochemical parameters of mild steel in the presence of PTT in 0.5M H<sub>2</sub>SO<sub>4</sub> solution deduced from EIS data

Conc. (mM)	R <sub>s</sub> (Ω cm <sup>2</sup> )	R <sub>ct</sub> (Ω cm <sup>2</sup> )	α	Y <sub>0</sub> × 10 <sup>4</sup> (S <sup>n</sup> Ω <sup>-1</sup> cm <sup>-2</sup> )	C <sub>dl</sub> , (μ F cm <sup>-2</sup> )	IE (%)
0.5M H <sub>2</sub> SO <sub>4</sub>	3.659	7.584	0.866	5.804	251.2	–
0.1	2.932	21.54	0.881	3.349	172.3	64.79
0.2	3.109	30.61	0.892	1.892	101.4	75.22
0.3	4.223	37.86	0.902	1.397	79.04	79.97
0.4	5.887	67.06	0.892	1.357	76.86	88.69
0.5	5.046	87.49	0.898	1.317	69.5	91.33

**Table 2.** Electrochemical parameters of mild steel in the presence of PTT in combination with 0.2% of KI in 0.5M H<sub>2</sub>SO<sub>4</sub> solution deduced from EIS data

Conc. (mM)	R <sub>s</sub> (Ω cm <sup>2</sup> )	R <sub>ct</sub> (Ω cm <sup>2</sup> )	α	Y <sub>0</sub> × 10 <sup>4</sup> (S <sup>n</sup> Ω <sup>-1</sup> cm <sup>-2</sup> )	C <sub>dl</sub> , (μ F cm <sup>-2</sup> )	IE (%)
0.1	3.031	32.23	0.874	2.531	126.4	76.47
0.2	5.531	69.51	0.888	1.376	88.44	89.09
0.3	4.698	87.47	0.899	1.316	79.56	91.33
0.4	4.222	123.8	0.883	1.228	73.57	93.87
0.5	3.340	203.6	0.874	1.092	63.02	96.27

**Table 3.** Potentiodynamic polarization parameters for corrosion of mild steel in 0.5M H<sub>2</sub>SO<sub>4</sub> with various concentrations of PTT in the absence and presence of 0.2% KI at 303 K

Conc. (mM)	Conc. KI (%)	E <sub>corr</sub> (mV vs SCE)	I <sub>corr</sub> (μA/cm <sup>2</sup> )	β <sub>c</sub> (mV/dec)	β <sub>a</sub> (mV/dec)	IE (%)
Blank	–	-482	3463	261.5	152.2	----
0.1	–	-572	776	205.2	117.3	77.6
0.1	0.2	-517	363	180.9	93.9	89.5
0.2	–	-558	653	167.7	102.6	81.1
0.2	0.2	-549	280	148.6	85.2	91.9
0.3	–	-564	422	147.0	91.3	87.8
0.3	0.2	-539	157	133.3	76.5	95.4
0.4	–	-540	369	167.5	101.0	89.3
0.4	0.2	-506	122	111.6	104.7	96.5
0.5	–	-516	292	181.9	95.5	91.6
0.5	0.2	-497	80	142.6	41.2	97.7

**Table 4.** Corrosion parameters obtained from weight loss measurements for mild steel in 0.5 M H<sub>2</sub>SO<sub>4</sub> containing various concentrations of PTT in the presence of 0.2 % KI at 303K

Conc. PTT (mM)	Conc. KI (%)	CR (mg cm <sup>-2</sup> h <sup>-1</sup> )	IE (%)
0.1	–	1.5421	61.07
0.1	0.2	1.0158	74.36
0.2	–	1.1141	71.88
0.2	0.2	0.3837	90.31
0.3	–	0.8239	79.20
0.3	0.2	0.2970	92.50
0.4	–	0.4772	85.95
0.4	0.2	0.2169	94.52
0.5	–	0.3318	91.62
0.5	0.2	0.1047	97.36

**Table 5.** Effect of immersion time on inhibitor performance for mild steel in 0.5M H<sub>2</sub>SO<sub>4</sub> at 303 K for 0.4 mM and 0.5 mM PTT

Immersion time (min)	IE (%)	
	0.5 mM PTT	0.5 mM PTT + 0.2% KI
60	91.62	97.36
120	89.94	95.21
180	86.97	92.53
240	85.29	90.96
360	81.42	86.37
1440	61.77	65.71

**Table 6.** Inhibition efficiency for different concentrations of KI for mild steel in 0.5 M H<sub>2</sub>SO<sub>4</sub> in the presence of 0.5 mM PTT at 303 K

KI (%)	IE (%)
0.05	94.78
0.1	95.24
0.15	96.24
0.2	97.36
0.25	97.30
0.3	95.52

**Table 7.** Values of synergism parameters (S) for different concentrations of PTT

Conc. PTT (mM)	S
0.1	0.76
0.2	1.45
0.3	1.39
0.4	1.10
0.5	1.73

**Table 8.** Effect of temperature on the inhibition efficiency *IE* (%) obtained from weight loss measurements

Temperature (K)	IE (%)	
	PTT (0.5 mM)	PTT (0.5 mM) + KI 0.2 %
298	88.84	95.88
303	91.62	97.36
308	90.82	94.83
313	89.05	90.37
323	76.04	90.35

**Table 9.** Thermodynamic activation parameters for mild steel in 0.5 M H<sub>2</sub>SO<sub>4</sub> solution and in the presence of PTT and (PTT+KI) obtained from weight loss measurements

	E <sub>a</sub> (kJ mol <sup>-1</sup> )	ΔH* (kJ mol <sup>-1</sup> )	ΔS*(J mol <sup>-1</sup> K <sup>-1</sup> )
0.5 M H <sub>2</sub> SO <sub>4</sub> (Blank)	55.83	53.4	-57.92
0.5 mM PTT	81.23	79.35	7.97
0.5 mM PTT + 0.2% KI	94.28	91.84	42.53

**Table 10.** Molecular properties of PTT obtained from the optimized structure using DFT at the B3LYP/6-31G

inhibitor	E <sub>HOMO</sub> (eV)	E <sub>LUMO</sub> (eV)	ΔE (eV)	μ (Debye)	I (eV)	A (eV)	χ (eV)	η (eV)	σ (eV <sup>-1</sup> )	ω (eV)	ΔN (eV)
PTT	-7,731	-0.260	7.471	4.381	7,731	0.260	3.996	3.736	0.268	2.137	0.402

**Table 11.** Molecular properties of PTT obtained from the optimized structure using DFT at the B3LYP/6-31G

Atoms	Mulliken charges
N1	-0.301
N2	0.125
C3	0.404
N4	-0.080
C5	-0.026
C6	0.832
C7	-0.040
C8	-0.533
C9	-0.171
C10	-0.311
C11	-0.595
S	-0.484
H1	0.112
H2	0.285
H3	0.208
H4	0.171
H5	0.156
H6	0.171
H7	0.076

#### 4. Conclusions

The inhibition behavior of PTT and its synergistic effect with KI for mild steel in 0.5 M H<sub>2</sub>SO<sub>4</sub> has been studied. The following conclusions may be drawn:

- PTT showed excellent inhibition properties for the corrosion of mild steel in 0.5 M H<sub>2</sub>SO<sub>4</sub> solution. The inhibition efficiency of PTT increased with the concentration and reached a maximum of 91.6% at 0.5 mM.
- Changes in impedance parameters were indicative of adsorption of PTT on the metal surface.
- PTT acts as a mixed-type inhibitor retarding the

anodic and cathodic corrosion reactions with predominant effect on the cathodic reaction.

- The inhibition efficiency *IE*% of PTT decreased with increasing temperature and its addition led to increase of the activation corrosion energy.
- Adsorption of PTT alone and in combination with KI on the mild steel surface obeys Langmuir's adsorption isotherm. The calculated value of Δ*G*<sup>o</sup><sub>ads</sub> obtained from the study indicates that PTT is adsorbed chemically and physically on steel surface in 0.5M H<sub>2</sub>SO<sub>4</sub> solution. The compound is adsorbed with the heteroatoms forming donor-acceptor bonds between unpaired electrons of the

heteroatoms and the active centers of the metal surface.

- Synergistic effects between PTT and KI were observed. The addition of KI to the solution enhanced the inhibition efficiency of PTT significantly. The adsorption of PTT is stabilized by the presence of iodide ions in 0.5 M H<sub>2</sub>SO<sub>4</sub>.
- The inhibitor efficiencies determined by polarization, EIS, and weight loss methods are in good agreement.
- SEM micrographs of mild steel specimens showed that the inhibitor molecules form a good protective film on the metal surface.
- The values of free energy of adsorption and the calculated quantum chemical suggest that the inhibition behavior of this triazole derivative involves two types of interaction, chemisorption and physisorption.
- Theoretical calculations provide good support to the experimental results.

## References

- [1] I. Ahamad, R. Prasad, M.A. Quraishi, Inhibition of mild steel corrosion in acid solution by Pheniramine drug: Experimental and theoretical study, *Corrosion Science*, 52 (2010) 3033-3041. <https://doi.org/10.1016/j.corsci.2010.05.022>
- [2] R.J. Aziz, Study of some drugs as corrosion inhibitors for mild steel in 1 MH<sub>2</sub>so<sub>4</sub> solution, *Int. J. Curr. Res. Chem. Pharm. Sci*, 3 (2016) 1-7. DOI:10.22192/ijcrpcps
- [3] L. Bammou, M. Belkhaouda, R. Salghi, O. Benali, A. Zarrouk, S. Al-Deyab, I. Warad, H. Zarrok, B. Hammouti, Effect of Harmal Extract on the Corrosion of C-steel in Hydrochloric Solution, *Int. J. Electrochem. Sci*, 9 (2014) 1506-1521
- [4] A.S. Fouda, A.S. Ellithy, Inhibition effect of 4-phenylthiazole derivatives on corrosion of 304L stainless steel in HCl solution, *Corrosion Science*, 51 (2009) 868-875. <https://doi.org/10.1016/j.corsci.2009.01.011>.
- [5] M. Gopiraman, N. Selvakumaran, D. Kesavan, I.S. Kim, R. Karvembu, Chemical and physical interactions of 1-benzoyl-3, 3-disubstituted thiourea derivatives on mild steel surface: corrosion inhibition in acidic media, *Industrial & Engineering Chemistry Research*, 51 (2012) 7910-7922. DOI: 10.1021/ie300048t
- [6] A. James, N. Oforka, O.K. Abiola, Inhibition of acid corrosion of mild steel by pyridoxal and pyridoxol hydrochlorides, *International Journal of Electrochemical Science*, 2 (2007) 278-284
- [7] M. Jeeva, G.V. Prabhu, M.S. Boobalan, C.M. Rajesh, Interactions and inhibition effect of urea-derived Mannich bases on a mild steel surface in HCl, *The Journal of Physical Chemistry C*, 119 (2015) 22025-22043. DOI: 10.1016/j.corsci.2010.05.022
- [8] P. Kamble, R. Dubey, Study of 1, 2, 4-Triazole As Effective Corrosion Inhibitor For Mild Steel Used In Oil And Gas Industries In 1M HCl, DOI (2018)
- [9] Y. Karzazi, M.E.A. Belghiti, A. Dafali, B. Hammouti, A theoretical investigation on the corrosion inhibition of mild steel by piperidine derivatives in hydrochloric acid solution, *J. Chem. Pharm. Res*, 6 (2014) 689-696. DOI: 10.22099/IJSTS.2015.3156
- [10] S. Kertit, B. Hammouti, Corrosion inhibition of iron in 1M HCl by 1-phenyl-5-mercapto-1, 2, 3, 4-tetrazole, *Applied Surface Science*, 93 (1996) 59-66. [https://doi.org/10.1016/0169-4332\(95\)00189-1](https://doi.org/10.1016/0169-4332(95)00189-1)
- [11] M.A. Amin, K.F. Khaled, Q. Mohsen, H.A. Arida, A study of the inhibition of iron corrosion in HCl solutions by some amino acids, *Corrosion Science*, 52 (2010) 1684-1695. <https://doi.org/10.1016/j.corsci.2010.01.019>
- [12] M. Dehdab, M. Shahraki, S.M. Habibi-Khorassani, Inhibitory effect of some benzothiazole derivatives on corrosion of mild steel: A computational study, *Iranian Journal of Science and Technology (Sciences)*, 39 (2015) 311-324. [10.22099/ijsts.2015.3156](https://doi.org/10.22099/ijsts.2015.3156)
- [13] P.A. Schweitzer, *Corrosion of Linings & Coatings: Cathodic and Inhibitor Protection and Corrosion Monitoring*, CRC press 2006.
- [14] C.M. Goulart, A. Esteves-Souza, C.A. Martinez-Huitle, C.J.F. Rodrigues, M.A.M. Maciel, A. Echevarria, Experimental and theoretical evaluation of semicarbazones and thiosemicarbazones as organic corrosion inhibitors, *Corrosion Science*, 67 (2013) 281-291. <https://doi.org/10.1016/j.corsci.2012.10.029>
- [15] A. Aouniti, H. Elmsellem, S. Tighadouini, M. Elazzouzi, S. Radi, A. Chetouani, B. Hammouti, A. Zarrouk, Schiff's base derived from 2-acetyl thiophene as corrosion inhibitor of steel in acidic medium, *Journal of Taibah University for Science*, 10 (2016) 774-785. [10.1016/j.jtusci.2015.11.008](https://doi.org/10.1016/j.jtusci.2015.11.008)
- [16] A. Yurt, B. Duran, H. Dal, An experimental and theoretical investigation on adsorption properties of some diphenolic Schiff bases as corrosion inhibitors at acidic solution/mild steel interface, *Arabian Journal of Chemistry*, 7 (2014) 732-740
- [17] J.O.M. Bockris, B.E. Conway, R.E. White, *Modern aspects of electrochemistry*, Springer Science & Business Media 2012.
- [18] P.A. Schweitzer, *Fundamentals of corrosion: mechanisms, causes, and preventative methods*, CRC Press 2009.

- [19] E.A. Noor, The inhibition of mild steel corrosion in phosphoric acid solutions by some N-heterocyclic compounds in the salt form, *Corrosion Science*, 47 (2005) 33-55
- [20] G. Avci, Inhibitor effect of N, N'-methylenediacrylamide on corrosion behavior of mild steel in 0.5 M HCl, *Materials Chemistry and Physics*, 112 (2008) 234-238
- [21] S.K. Shukla, M.A. Quraishi, Cefotaxime sodium: A new and efficient corrosion inhibitor for mild steel in hydrochloric acid solution, *Corrosion Science*, 51 (2009) 1007-1011. <https://doi.org/10.1016/j.corsci.2009.02.024>
- [22] F.S. de Souza, A. Spinelli, Caffeic acid as a green corrosion inhibitor for mild steel, *Corrosion Science*, 51 (2009) 642-649. <https://doi.org/10.1016/j.corsci.2008.12.013>
- [23] Y. El Aoufir, J. Sebhaoui, H. Lgaz, Y. El Bakri, A. Zarrouk, F. Bentiss, H. Oudda, Corrosion inhibition of carbon steel in 1 M HCl by 1, 5-benzodiazepine derivative: Experimental and molecular modeling studies, *Journal of Materials and Environmental Science*, 8 (2017) 2161-2173
- [24] N. Kovačević, A. Kokalj, Chemistry of the interaction between azole type corrosion inhibitor molecules and metal surfaces, *Materials Chemistry and Physics*, 137 (2012) 331-339. <https://doi.org/10.1016/j.matchemphys.2012.09.030>
- [25] M.A. Quraishi, R. Sardar, D. Jamal, Corrosion inhibition of mild steel in hydrochloric acid by some aromatic hydrazides, *Materials Chemistry and Physics*, 71 (2001) 309-313. [https://doi.org/10.1016/S0254-0584\(01\)00295-4](https://doi.org/10.1016/S0254-0584(01)00295-4)
- [26] E. Sadeghi Meresht, T. Shahrabi Farahani, J. Neshati, 2-Butyne-1,4-diol as a novel corrosion inhibitor for API X65 steel pipeline in carbonate/bicarbonate solution, *Corrosion Science*, 54 (2012) 36-44. <https://doi.org/10.1016/j.corsci.2011.08.052>
- [27] M. Gopiraman, N. Selvakumaran, D. Kesavan, R. Karvembu, Adsorption and corrosion inhibition behaviour of N-(phenylcarbamothioyl)benzamide on mild steel in acidic medium, *Progress in Organic Coatings*, 73 (2012) 104-111. <https://doi.org/10.1016/j.porgcoat.2011.09.006>
- [28] B.D. Mert, M. Erman Mert, G. Kardaş, B. Yazıcı, Experimental and theoretical investigation of 3-amino-1,2,4-triazole-5-thiol as a corrosion inhibitor for carbon steel in HCl medium, *Corrosion Science*, 53 (2011) 4265-4272. <https://doi.org/10.1016/j.corsci.2011.08.038>
- [29] H.-L. Wang, R.-B. Liu, J. Xin, Inhibiting effects of some mercapto-triazole derivatives on the corrosion of mild steel in 1.0 M HCl medium, *Corrosion Science*, 46 (2004) 2455-2466. <https://doi.org/10.1016/j.corsci.2004.01.023>
- [30] L. Wang, Inhibition of mild steel corrosion in phosphoric acid solution by triazole derivatives, *Corrosion Science*, 48 (2006) 608-616. <https://doi.org/10.1016/j.corsci.2005.02.007>
- [31] A.Y. Musa, A.A.H. Kadhun, A.B. Mohamad, M.S. Takriff, A.R. Daud, S.K. Kamarudin, On the inhibition of mild steel corrosion by 4-amino-5-phenyl-4H-1, 2, 4-triazole-3-thiol, *Corrosion Science*, 52 (2010) 526-533. <https://doi.org/10.1016/j.corsci.2009.10.009>
- [32] M.L. Zheludkevich, K.A. Yasakau, S.K. Poznyak, M.G.S. Ferreira, Triazole and thiazole derivatives as corrosion inhibitors for AA2024 aluminium alloy, *Corrosion Science*, 47 (2005) 3368-3383. <https://doi.org/10.1016/j.corsci.2005.05.040>
- [33] M.-J.Z. Lin Wang, Fa-Chang Yang, and Cheng-Wei Gao, Study of a Triazole Derivative as Corrosion Inhibitor for Mild Steel in Phosphoric Acid Solution, *International Journal of Corrosion*, 2012 (2012). [10.1155/2012/573964](https://doi.org/10.1155/2012/573964)
- [34] M. Messali, M. Larouj, H. Lgaz, N. Rezki, F.F. Al-Blewi, M.R. Aouad, A. Chaouiki, R. Salghi, I.-M. Chung, A new schiff base derivative as an effective corrosion inhibitor for mild steel in acidic media: Experimental and computer simulations studies, *Journal of Molecular Structure*, 1168 (2018) 39-48. <https://doi.org/10.1016/j.molstruc.2018.05.018>
- [35] Y. Elkhofī, I. Forsal, E. Rakib, B. Mernari, Optimization of the Inhibitor Efficiency of a Triazole on Corrosion of Mild Steel in 1M HCl, *Journal of Advanced Electrochemistry*, DOI (2017) 141-143
- [36] Q. Ma, S. Qi, X. He, Y. Tang, G. Lu, 1,2,3-Triazole derivatives as corrosion inhibitors for mild steel in acidic medium: Experimental and computational chemistry studies, *Corrosion Science*, 129 (2017) 91-101. <https://doi.org/10.1016/j.corsci.2017.09.025>
- [37] M. Tourabi, A. Sahibed-dine, A. Zarrouk, I.B. Obot, B. Hammouti, F. Bentiss, A. Nahlé, 3,5-Diaryl-4-amino-1,2,4-triazole derivatives as effective corrosion inhibitors for mild steel in hydrochloric acid solution: Correlation between anti-corrosion activity and chemical structure, *Protection of Metals and Physical Chemistry of Surfaces*, 53 (2017) 548-559. [10.1134/s2070205117030236](https://doi.org/10.1134/s2070205117030236)
- [38] M.E. Belghiti, Y. Karzazi, A. Dafali, I.B. Obot, E.E. Ebenso, K.M. Emran, I. Bahadur, B.

- Hammouti, F. Bentiss, Anti-corrosive properties of 4-amino-3,5-bis(disubstituted)-1,2,4-triazole derivatives on mild steel corrosion in 2M H<sub>3</sub>PO<sub>4</sub> solution: Experimental and theoretical studies, *Journal of Molecular Liquids*, 216 (2016) 874-886. <https://doi.org/10.1016/j.molliq.2015.12.093>
- [39] M. ElBelghiti, Y. Karzazi, A. Dafali, B. Hammouti, F. Bentiss, I.B. Obot, I. Bahadur, E.E. Ebenso, Experimental, quantum chemical and Monte Carlo simulation studies of 3,5-disubstituted-4-amino-1,2,4-triazoles as corrosion inhibitors on mild steel in acidic medium, *Journal of Molecular Liquids*, 218 (2016) 281-293. <https://doi.org/10.1016/j.molliq.2016.01.076>
- [40] M.K. Pavithra, T.V. Venkatesha, K. Vathsala, K.O. Nayana, Synergistic effect of halide ions on improving corrosion inhibition behaviour of benzisothiazole-3-piperazine hydrochloride on mild steel in 0.5M H<sub>2</sub>SO<sub>4</sub> medium, *Corrosion Science*, 52 (2010) 3811-3819. <https://doi.org/10.1016/j.corsci.2010.07.034>
- [41] M. El Azhar, B. Mernari, M. Traisnel, F. Bentiss, M. Lagrenée, Corrosion inhibition of mild steel by the new class of inhibitors [2,5-bis(n-pyridyl)-1,3,4-thiadiazoles] in acidic media, *Corrosion Science*, 43 (2001) 2229-2238. [https://doi.org/10.1016/S0010-938X\(01\)00034-8](https://doi.org/10.1016/S0010-938X(01)00034-8)
- [42] E.E. Oguzie, Y. Li, F.H. Wang, Corrosion inhibition and adsorption behavior of methionine on mild steel in sulfuric acid and synergistic effect of iodide ion, *Journal of Colloid and Interface Science*, 310 (2007) 90-98. <https://doi.org/10.1016/j.jcis.2007.01.038>
- [43] P.C. Okafor, Y. Zheng, Synergistic inhibition behaviour of methylbenzyl quaternary imidazoline derivative and iodide ions on mild steel in H<sub>2</sub>SO<sub>4</sub> solutions, *Corrosion Science*, 51 (2009) 850-859. <https://doi.org/10.1016/j.corsci.2009.01.027>
- [44] C. Jeyaprabha, S. Sathiyarayanan, G. Venkatachari, Co-adsorption effect of polyaniline and halide ions on the corrosion of iron in 0.5M H<sub>2</sub>SO<sub>4</sub> solutions, *Journal of Electroanalytical Chemistry*, 583 (2005) 232-240. <https://doi.org/10.1016/j.jelechem.2005.06.006>
- [45] S.S.A. Rehim, O.A. Hazzazi, M.A. Amin, K.F. Khaled, On the corrosion inhibition of low carbon steel in concentrated sulphuric acid solutions. Part I: Chemical and electrochemical (AC and DC) studies, *Corrosion Science*, 50 (2008) 2258-2271. <https://doi.org/10.1016/j.corsci.2008.06.005>
- [46] C. Jeyaprabha, S. Sathiyarayanan, G. Venkatachari, Influence of halide ions on the adsorption of diphenylamine on iron in 0.5M H<sub>2</sub>SO<sub>4</sub> solutions, *Electrochimica Acta*, 51 (2006) 4080-4088. <https://doi.org/10.1016/j.electacta.2005.11.026>
- [47] F. Bentiss, M. Bouanis, B. Mernari, M. Traisnel, M. Lagrenée, Effect of iodide ions on corrosion inhibition of mild steel by 3,5-bis(4-methylthiophenyl)-4H-1,2,4-triazole in sulfuric acid solution, *Journal of Applied Electrochemistry*, 32 (2002) 671-678. <https://doi.org/10.1023/a:1020161332235>
- [48] S. Rajendran, B.V. Apparao, N. Palaniswamy, Synergistic and antagonistic effects existing among polyacrylamide, phenyl phosphonate and Zn<sup>2+</sup> on the inhibition of corrosion of mild steel in a neutral aqueous environment, *Electrochimica Acta*, 44 (1998) 533-537. [https://doi.org/10.1016/S0013-4686\(98\)00079-6](https://doi.org/10.1016/S0013-4686(98)00079-6)
- [49] E.E. Ebenso, Synergistic effect of halide ions on the corrosion inhibition of aluminium in H<sub>2</sub>SO<sub>4</sub> using 2-acetylphenothiazine, *Materials Chemistry and Physics*, 79 (2003) 58-70. [https://doi.org/10.1016/S0254-0584\(02\)00446-7](https://doi.org/10.1016/S0254-0584(02)00446-7)
- [50] D. Turcio-Ortega, T. Pandiyan, J. Cruz, E. Garcia-Ochoa, Interaction of Imidazoline Compounds with Fe (n = 1-4 Atoms) as a Model for Corrosion Inhibition: DFT and Electrochemical Studies, *The Journal of Physical Chemistry C*, 111 (2007) 9853-9866. <https://doi.org/10.1021/jp0711038>
- [51] H. Ju, X. Li, N. Cao, F. Wang, Y. Liu, Y. Li, Schiff-base derivatives as corrosion inhibitors for carbon steel materials in acid media: quantum chemical calculations, *Corrosion Engineering, Science and Technology*, 53 (2018) 36-43. <https://doi.org/10.1080/1478422x.2017.1368216>
- [52] L. Guo, S. Zhu, S. Zhang, Q. He, W. Li, Theoretical studies of three triazole derivatives as corrosion inhibitors for mild steel in acidic medium, *Corrosion Science*, 87 (2014) 366-375. <https://doi.org/10.1016/j.corsci.2014.06.040>
- [53] K.R. Ansari, M.A. Qurashi, A. Singh, Schiff's base of pyridyl substituted triazoles as new and effective corrosion inhibitors for mild steel in hydrochloric acid solution, *Corrosion Science*, 79 (2014) 5-15. <https://doi.org/10.1016/j.corsci.2013.10.009>
- [54] N. Yilmaz, A. Fitoz, Y. Ergun, K.C. Emregül, A combined electrochemical and theoretical study into the effect of 2-((thiazole-2-ylimino)methyl)phenol as a corrosion inhibitor for mild steel in a highly acidic environment, *Corrosion Science*, 111 (2016) 110-120. <https://doi.org/10.1016/j.corsci.2016.05.002>
- [55] J.W. MacDonald, D.M. McKinnon, 1,2,4-Dithiazole-3-thiones and derivatives, *Canadian*

- Journal of Chemistry, 45 (1967) 1225-1229.10.1139/v67-202
- [56] M. Amir, K. Shikha, Synthesis and anti-inflammatory, analgesic, ulcerogenic and lipid peroxidation activities of some new 2-[(2,6-dichloroanilino) phenyl]acetic acid derivatives, *European Journal of Medicinal Chemistry*, 39 (2004) 535-545. <https://doi.org/10.1016/j.ejmech.2004.02.008>
- [57] R. Agrawal, S. Pancholi, Synthesis, characterization and evaluation of antimicrobial activity of a series of 1, 2, 4-triazoles, *Der Pharma Chemica*, 3 (2011) 32-40
- [58] M. Amini, M. Aliofkhaezai, A.N. Kashani, A.S. Rouhaghdam, Mild Steel Corrosion Inhibition by Benzotriazole in 0.5 M Sulfuric Acid Solution on Rough and Smooth Surfaces, *Int. J. Electrochem. Sci*, 12 (2017) 8708-8732
- [59] M. Prajila, A. Joseph, Controlling the Rate of Dissolution of Mild Steel in Sulfuric Acid Through the Adsorption and Inhibition Characteristics of (4-(4-Hydroxybenzylideneamino)-4H-1,2,4-Triazole-3,5-diyl)dimethanol (HATD), *Journal of Bio- and Tribo-Corrosion*, 3 (2017) 10.1007/s40735-016-0070-z
- [60] A. Espinoza-Vázquez, G.E. Negrón-Silva, R. González-Olvera, D. Angeles-Beltrán, M. Romero-Romo, M. Palomar-Pardavé, Effect of Hydrodynamic Conditions, Temperature and Immersion Times on the Corrosion Inhibition Efficiency of API 5L X52 Steel in 1M HCl Containing 1H-1,2,4 or 1H-1,2,3-triazoles, *Arabian Journal for Science and Engineering*, 42 (2017) 163-174.10.1007/s13369-016-2116-4
- [61] H. Debab, T. Douadi, D. Daoud, S. Issaadi, S. Chafaa, Electrochemical and Quantum Chemical Studies of Adsorption and Corrosion Inhibition of Two New Schiff Bases on Carbon Steel in Hydrochloric Acid Media, *International Journal of Electrochemical Science*, 13 (2018) 6958-6977
- [62] S.E. Hachani, Z. Necira, D.E. Mazouzi, N. Nebbache, Understanding the Inhibition of Mild Steel Corrosion by dianiline Schiff bases: a DFT investigation, 2018, 65 (2018) 8.10.17344/acs.2017.3803
- [63] R.A. Gaussian09, 1, MJ Frisch, GW Trucks, HB Schlegel, GE Scuseria, MA Robb, JR Cheeseman, G. Scalmani, V. Barone, B. Mennucci, GA Petersson et al., Gaussian, Inc., Wallingford CT, 121 (2009) 150-166
- [64] A. Wagner, R. Flaig, D. Zobel, B. Dittrich, P. Bombicz, M. Strümpel, P. Luger, T. Koritsanszky, H.-G. Krane, Structure and Charge Density of a C60-Fullerene Derivative Based on a High Resolution Synchrotron Diffraction Experiment at 100 K, *The Journal of Physical Chemistry A*, 106 (2002) 6581-6590.10.1021/jp0145199
- [65] J.M. Bowman, B.J. Braams, S. Carter, C. Chen, G. Czako, B. Fu, X. Huang, E. Kamarchik, A.R. Sharma, B.C. Shepler, Y. Wang, Z. Xie, Ab-Initio-Based Potential Energy Surfaces for Complex Molecules and Molecular Complexes, *The Journal of Physical Chemistry Letters*, 1 (2010) 1866-1874.10.1021/jz100626h
- [66] L. Boucherit, T. Douadi, N. Chafai, M. Al-Noaimi, S. Chafaa, The inhibition Activity of 1, 10-bis (2-formylphenyl)-1, 4, 7, 10-tetraoxadecane (Ald) and its Schiff base (L) on the Corrosion of Carbon Steel in HCl: Experimental and Theoretical Studies, *Int. J. Electrochem. Sci*, 13 (2018) 3997-4025
- [67] Y. Bellal, S. Keraghel, F. Benghanem, T. Linda, G. Sığircık, B. Riadh, A. Ourari, A New Inhibitor for Steel Rebar Corrosion in Concrete: Electrochemical and Theoretical Studies, *International Journal of Electrochemical Science*, 13 (2018) 7218-7245
- [68] R.G. Parr, R.G. Pearson, Absolute hardness: companion parameter to absolute electronegativity, *Journal of the American Chemical Society*, 105 (1983) 7512-7516.10.1021/ja00364a005
- [69] H. Allal, Y. Belhocine, E. Zouaoui, Computational study of some thiophene derivatives as aluminium corrosion inhibitors, *Journal of Molecular Liquids*, 265 (2018) 668-678. <https://doi.org/10.1016/j.molliq.2018.05.099>
- [70] I. Belfilali, A. Chetouani, B. Hammouti, S. Louhibi, A. Aouniti, S.S. Al-Deyab, Quantum chemical study of inhibition of the corrosion of mild steel in 1 M hydrochloric acid solution by newly synthesized benzamide derivatives, *Research on Chemical Intermediates*, 40 (2014) 1069-1088.10.1007/s11164-013-1022-6
- [71] L.H. Madkour, S.K. Elroby, Inhibitive properties, thermodynamic, kinetics and quantum chemical calculations of polydentate Schiff base compounds as corrosion inhibitors for iron in acidic and alkaline media, *International Journal of Industrial Chemistry*, 6 (2015) 165-184.10.1007/s40090-015-0039-7
- [72] D. Daoud, T. Douadi, H. Hamani, S. Chafaa, M. Al-Noaimi, Corrosion inhibition of mild steel by two new S-heterocyclic compounds in 1 M HCl: Experimental and computational study, *Corrosion Science*, 94 (2015) 21-37. <https://doi.org/10.1016/j.corsci.2015.01.025>
- [73] F. Mansfeld, M.W. Kendig, S. Tsai, Evaluation of Corrosion Behavior of Coated Metals with AC

- Impedance Measurements, *CORROSION*, 38 (1982) 478-485.10.5006/1.3577363
- [74] F. Mansfeld, Discussion: Electrochemical Techniques for Studying Corrosion of Reinforcing Steel: Limitations and Advantages, *CORROSION*, 61 (2005) 739-742.10.5006/1.3281682
- [75] X.Y. Wang, J. Yan, H.T. Yuan, Y.S. Zhang, D.Y. Song, Impedance studies of nickel hydroxide microencapsulated by cobalt, *International Journal of Hydrogen Energy*, 24 (1999) 973-980.https://doi.org/10.1016/S0360-3199(98)00130-X
- [76] M.S. Morad, Corrosion inhibition of mild steel in sulfamic acid solution by S-containing amino acids, *Journal of Applied Electrochemistry*, 38 (2008) 1509-1518.10.1007/s10800-008-9595-2
- [77] E.A. Noor, Evaluation of inhibitive action of some quaternary N-heterocyclic compounds on the corrosion of Al-Cu alloy in hydrochloric acid, *Materials Chemistry and Physics*, 114 (2009) 533-541.https://doi.org/10.1016/j.matchemphys.2008.09.065
- [78] P. Dohare, M. Quraishi, I. Obot, A combined electrochemical and theoretical study of pyridine-based Schiff bases as novel corrosion inhibitors for mild steel in hydrochloric acid medium, *Journal of Chemical Sciences*, 130 (2018) 8
- [79] Wu, Xiaojuan, H. Ma, S. Chen, Z. Xu, A. Sui, General Equivalent Circuits for Faradaic Electrode Processes under Electrochemical Reaction Control, *Journal of The Electrochemical Society*, 146 (1999) 1847-1853.10.1149/1.1391854
- [80] S. Deng, X. Li, Inhibition by Ginkgo leaves extract of the corrosion of steel in HCl and H<sub>2</sub>SO<sub>4</sub> solutions, *Corrosion Science*, 55 (2012) 407-415.https://doi.org/10.1016/j.corsci.2011.11.005
- [81] A.Y. Musa, R.T.T. Jalgham, A.B. Mohamad, Molecular dynamic and quantum chemical calculations for phthalazine derivatives as corrosion inhibitors of mild steel in 1M HCl, *Corrosion Science*, 56 (2012) 176-183.https://doi.org/10.1016/j.corsci.2011.12.005
- [82] J. Zhao, G. Chen, The synergistic inhibition effect of oleic-based imidazoline and sodium benzoate on mild steel corrosion in a CO<sub>2</sub>-saturated brine solution, *Electrochimica Acta*, 69 (2012) 247-255.https://doi.org/10.1016/j.electacta.2012.02.101
- [83] K.F. Khaled, K. Babić-Samarđžija, N. Hackerman, Cobalt(III) complexes of macrocyclic-bidentate type as a new group of corrosion inhibitors for iron in perchloric acid, *Corrosion Science*, 48 (2006) 3014-3034.https://doi.org/10.1016/j.corsci.2005.11.011
- [84] F. Bentiss, M. Traisnel, M. Lagrenee, The substituted 1,3,4-oxadiazoles: a new class of corrosion inhibitors of mild steel in acidic media, *Corrosion Science*, 42 (2000) 127-146.https://doi.org/10.1016/S0010-938X(99)00049-9
- [85] I.B. Obot, Synergistic Effect of Nizoral and Iodide Ions on the Corrosion Inhibition of Mild Steel in Sulphuric Acid Solution, *Portugaliae Electrochimica Acta*, 27 (2009) 539-553
- [86] E.S. Ferreira, C. Giacomelli, F.C. Giacomelli, A. Spinelli, Evaluation of the inhibitor effect of L-ascorbic acid on the corrosion of mild steel, *Materials Chemistry and Physics*, 83 (2004) 129-134.https://doi.org/10.1016/j.matchemphys.2003.09.020
- [87] A.A. Farag, M.A. Hegazy, Synergistic inhibition effect of potassium iodide and novel Schiff bases on X65 steel corrosion in 0.5M H<sub>2</sub>SO<sub>4</sub>, *Corrosion Science*, 74 (2013) 168-177.https://doi.org/10.1016/j.corsci.2013.04.039
- [88] O. Benali, L. Larabi, B. Tabti, Y. Harek, Influence of 1-methyl 2-mercapto imidazole on corrosion inhibition of carbon steel in 0.5 M H<sub>2</sub>SO<sub>4</sub>, *Anti-Corrosion Methods and Materials*, 52 (2005) 280-285.doi:10.1108/00035590510615776
- [89] L. Larabi, O. Benali, S.M. Mekelleche, Y. Harek, 2-Mercapto-1-methylimidazole as corrosion inhibitor for copper in hydrochloric acid, *Applied Surface Science*, 253 (2006) 1371-1378.https://doi.org/10.1016/j.apsusc.2006.02.013
- [90] O. Benali, L. Larabi, M. Traisnel, L. Gengembre, Y. Harek, Electrochemical, theoretical and XPS studies of 2-mercapto-1-methylimidazole adsorption on carbon steel in 1M HClO<sub>4</sub>, *Applied Surface Science*, 253 (2007) 6130-6139.https://doi.org/10.1016/j.apsusc.2007.01.075
- [91] S. Leelavathi, R. Rajalakshmi, Dodonaea viscosa (L.) Leaves extract as acid Corrosion inhibitor for mild Steel—A Green approach, *J Mater Environ Sci*, 4 (2013) 625-638
- [92] H. Ouici, O. Benali, Y. Harek, S. Al-Deyab, L. Larabi, B. Hammouti, Influence of the 2-Mercapto-1-Methyl Imidazole (MMI) on the Corrosion Inhibition of Mild Steel in 5% HCl, *Int. J. Electrochem. Sci*, 7 (2012) 2304-2319
- [93] I. Ahamad, C. Gupta, R. Prasad, M.A. Quraishi, An experimental and theoretical investigation of adsorption characteristics of a Schiff base compound as corrosion inhibitor at mild steel/hydrochloric acid interface, *Journal of Applied Electrochemistry*, 40 (2010) 2171-2183.10.1007/s10800-010-0199-2

- [94] I. Ahamad, R. Prasad, M.A. Quraishi, Adsorption and inhibitive properties of some new Mannich bases of Isatin derivatives on corrosion of mild steel in acidic media, *Corrosion Science*, 52 (2010) 1472-1481. <https://doi.org/10.1016/j.corsci.2010.01.015>
- [95] G.K. Gomma, Corrosion of low-carbon steel in sulphuric acid solution in presence of pyrazole—halides mixture, *Materials Chemistry and Physics*, 55 (1998) 241-246. [https://doi.org/10.1016/S0254-0584\(98\)00155-2](https://doi.org/10.1016/S0254-0584(98)00155-2)
- [96] D.-Q. Zhang, L.-X. Gao, G.-D. Zhou, Synergistic effect of 2-mercapto benzimidazole and KI on copper corrosion inhibition in aerated sulfuric acid solution, *Journal of Applied Electrochemistry*, 33 (2003) 361-366. [10.1023/a:1024403314993](https://doi.org/10.1023/a:1024403314993)
- [97] A. Ridhwan, A. Rahim, A. Shah, Synergistic effect of halide ions on the corrosion inhibition of mild steel in hydrochloric acid using mangrove tannin, *International Journal of Electrochemical Science*, 7 (2012) 8091-8104
- [98] S. Umoren, M. Solomon, Effect of halide ions additives on the corrosion inhibition of aluminum in HCl by polyacrylamide, *Arabian Journal for Science and Engineering*, 35 (2010) 115
- [99] E.E. Oguzie, A.I. Onuchukwu, P.C. Okafor, E.E. Ebenso, Corrosion inhibition and adsorption behaviour of Ocimum basilicum extract on aluminium, *Pigment & Resin Technology*, 35 (2006) 63-70. [doi:10.1108/03699420610652340](https://doi.org/10.1108/03699420610652340)
- [100] S.A. Umoren, M.M. Solomon, Effect of halide ions on the corrosion inhibition efficiency of different organic species – A review, *Journal of Industrial and Engineering Chemistry*, 21 (2015) 81-100. <https://doi.org/10.1016/j.jiec.2014.09.033>
- [101] L. Hamadi, S. Mansouri, K. Oulmi, A. Kareche, The use of amino acids as corrosion inhibitors for metals: A review, *Egyptian Journal of Petroleum*, DOI <https://doi.org/10.1016/j.ejpe.2018.04.004> (2018). <https://doi.org/10.1016/j.ejpe.2018.04.004>
- [102] O. Hazazi, A. Fawzy, M. Awad, Synergistic effect of halides on the corrosion inhibition of mild steel in H<sub>2</sub>SO<sub>4</sub> by a triazole derivative: kinetics and thermodynamic studies, *Int. J. Electrochem. Sci*, 9 (2014) 4086-4103
- [103] E.E. Ebenso, U.J. Ekpe, S.A. Umoren, E. Jackson, O.K. Abiola, N.C. Oforika, Synergistic effect of halide ions on the corrosion inhibition of aluminum in acidic medium by some polymers, *Journal of Applied Polymer Science*, 100 (2006) 2889-2894. [doi:10.1002/app.23505](https://doi.org/10.1002/app.23505)
- [104] E.E. Oguzie, Influence of halide ions on the inhibitive effect of congo red dye on the corrosion of mild steel in sulphuric acid solution, *Materials Chemistry and Physics*, 87 (2004) 212-217. <https://doi.org/10.1016/j.matchemphys.2004.06.006>
- [105] P.C. Okafor, V.I. Osabor, E.E. Ebenso, Eco-friendly corrosion inhibitors: inhibitive action of ethanol extracts of *Garcinia kola* for the corrosion of mild steel in H<sub>2</sub>SO<sub>4</sub> solutions, *Pigment & Resin Technology*, 36 (2007) 299-305. [doi:10.1108/03699420710820414](https://doi.org/10.1108/03699420710820414)
- [106] U.M. Eduok, S.A. Umoren, A.P. Udoh, Synergistic inhibition effects between leaves and stem extracts of *Sida acuta* and iodide ion for mild steel corrosion in 1M H<sub>2</sub>SO<sub>4</sub> solutions, *Arabian Journal of Chemistry*, 5 (2012) 325-337. <https://doi.org/10.1016/j.arabjc.2010.09.006>
- [107] K. Aramaki, N. Hackerman, Inhibition Mechanism of Medium-Sized Polymethyleneimine, *Journal of The Electrochemical Society*, 116 (1969) 568-574. [10.1149/1.2411965](https://doi.org/10.1149/1.2411965)
- [108] S.S. Azim, S. Muralidharan, S.V. Iyer, B. Muralidharan, T. Vasudevan, Synergistic influence of iodide ions on inhibition of corrosion of mild steel in H<sub>2</sub>SO<sub>4</sub> by N-phenyl thiourea, *British Corrosion Journal*, 33 (1998) 297-301. [10.1179/000705998798115326](https://doi.org/10.1179/000705998798115326)
- [109] A.K. Singh, M.A. Quraishi, Adsorption properties and inhibition of mild steel corrosion in hydrochloric acid solution by ceftobiprole, *Journal of Applied Electrochemistry*, 41 (2011) 7-18. [10.1007/s10800-010-0202-y](https://doi.org/10.1007/s10800-010-0202-y)
- [110] A.K. Singh, M.A. Quraishi, Investigation of the effect of disulfiram on corrosion of mild steel in hydrochloric acid solution, *Corrosion Science*, 53 (2011) 1288-1297. <https://doi.org/10.1016/j.corsci.2011.01.002>
- [111] P.N. Clark, E. Jackson, M. Robinson, Effect of Thiourea and Some of its Derivatives on the Corrosion Behaviour of Nickel in 50% v/v (5-6M) Hydrochloric Acid, *British Corrosion Journal*, 14 (1979) 33-39. [10.1179/000705979798275988](https://doi.org/10.1179/000705979798275988)
- [112] D.K. Yadav, M.A. Quraishi, B. Maiti, Inhibition effect of some benzylidenes on mild steel in 1M HCl: An experimental and theoretical correlation, *Corrosion Science*, 55 (2012) 254-266. <https://doi.org/10.1016/j.corsci.2011.10.030>
- [113] S. Muralidharan, M.A. Quraishi, S.V.K. Iyer, The effect of molecular structure on hydrogen permeation and the corrosion inhibition of mild steel in acidic solutions, *Corrosion Science*, 37 (1995) 1739-1750. [https://doi.org/10.1016/0010-938X\(95\)00068-U](https://doi.org/10.1016/0010-938X(95)00068-U)

- [114] A. Zarrouk, B. Hammouti, H. Zarrok, R. Salghi, A. Dafali, L. Bazzi, L. Bammou, S. Al-Deyab, Electrochemical impedance spectroscopy and weight loss study for new pyridazine derivative as inhibitor for copper in nitric acid, *Der Pharm, Chem*, 4 (2012) 337-346
- [115] B. Donnelly, T.C. Downie, R. Grzeskowiak, H.R. Hamburg, D. Short, The effect of electronic delocalization in organic groups R in substituted thiocarbamoyl RCSNH<sub>2</sub> and related compounds on inhibition efficiency, *Corrosion Science*, 18 (1978) 109-116. [https://doi.org/10.1016/S0010-938X\(78\)80081-X](https://doi.org/10.1016/S0010-938X(78)80081-X)
- [116] J.D. Talati, D.K. Gandhi, N-heterocyclic compounds as corrosion inhibitors for aluminium-copper alloy in hydrochloric acid, *Corrosion Science*, 23 (1983) 1315-1332. [https://doi.org/10.1016/0010-938X\(83\)90081-1](https://doi.org/10.1016/0010-938X(83)90081-1)
- [117] F.M. Donahue, K. Nobe, Theory of Organic Corrosion Inhibitors: Adsorption and Linear Free Energy Relationships, *Journal of The Electrochemical Society*, 112 (1965) 886-891. [10.1149/1.2423723](https://doi.org/10.1149/1.2423723)
- [118] A. Yurt, A. Balaban, S.U. Kandemir, G. Bereket, B. Erk, Investigation on some Schiff bases as HCl corrosion inhibitors for carbon steel, *Materials Chemistry and Physics*, 85 (2004) 420-426. <https://doi.org/10.1016/j.matchemphys.2004.01.033>
- [119] A.K. Singh, M.A. Quraishi, The effect of some bis-thiadiazole derivatives on the corrosion of mild steel in hydrochloric acid, *Corrosion Science*, 52 (2010) 1373-1385. <https://doi.org/10.1016/j.corsci.2010.01.007>
- [120] A.K. Singh, M.A. Quraishi, Inhibitive effect of diethylcarbamazine on the corrosion of mild steel in hydrochloric acid, *Corrosion Science*, 52 (2010) 1529-1535. <https://doi.org/10.1016/j.corsci.2009.12.011>
- [121] M. Dahmani, A. Et-Touhami, S. Al-Deyab, B. Hammouti, A. Bouyanzer, Corrosion inhibition of C38 steel in 1 M HCl: A comparative study of black pepper extract and its isolated piperine, *Int. J. Electrochem. Sci*, 5 (2010) 1060-1069
- [122] H. Allal, Y. Belhocine, E. Zouaoui, Computational study of some thiophene derivatives as aluminium corrosion inhibitors, *Journal of Molecular Liquids*, DOI (2018)
- [123] N. Zulfareen, T. Venugopal, K. Kannan, Experimental and Theoretical Studies on the Corrosion Inhibition of Brass in Hydrochloric Acid by N-(4-((4-Benzhydryl Piperazin-1-yl) Methyl Carbamoyl) Phenyl) Furan-2-Carboxamide, *International Journal of Corrosion*, 2018 (2018) 18.10.1155/2018/9372804
- [124] D.B. Hmamou, R. Salghi, A. Zarrouk, M.R. Aouad, O. Benali, H. Zarrok, M. Messali, B. Hammouti, M.M. Kabanda, M. Bouachrine, E.E. Ebenso, Weight Loss, Electrochemical, Quantum Chemical Calculation, and Molecular Dynamics Simulation Studies on 2-(Benzylthio)-1,4,5-triphenyl-1H-imidazole as an Inhibitor for Carbon Steel Corrosion in Hydrochloric Acid, *Industrial & Engineering Chemistry Research*, 52 (2013) 14315-14327. [10.1021/ie401034h](https://doi.org/10.1021/ie401034h)
- [125] A.-R. Allouche, Gabedit—A graphical user interface for computational chemistry softwares, *Journal of Computational Chemistry*, 32 (2011) 174-182. [doi:10.1002/jcc.21600](https://doi.org/10.1002/jcc.21600)
- [126] M.A. Bedair, M.M.B. El-Sabbah, A.S. Fouda, H.M. Elaryian, Synthesis, electrochemical and quantum chemical studies of some prepared surfactants based on azodye and Schiff base as corrosion inhibitors for steel in acid medium, *Corrosion Science*, 128 (2017) 54-72. <https://doi.org/10.1016/j.corsci.2017.09.016>
- [127] R.K. Gupta, M. Malviya, C. Verma, M.A. Quraishi, Aminoazobenzene and diaminoazobenzene functionalized graphene oxides as novel class of corrosion inhibitors for mild steel: Experimental and DFT studies, *Materials Chemistry and Physics*, 198 (2017) 360-373. <https://doi.org/10.1016/j.matchemphys.2017.06.030>
- [128] H.F. Finley, N. Hackerman, Effect of Adsorption of Polar Organic Compounds on the Reactivity of Steel, *Journal of The Electrochemical Society*, 107 (1960) 259-263. [10.1149/1.2427675](https://doi.org/10.1149/1.2427675)
- [129] A.S. Fouda, G.Y. Elewady, K. Shalabi, H.K. Abd El-Aziz, Alcamines as corrosion inhibitors for reinforced steel and their effect on cement based materials and mortar performance, *RSC Advances*, 5 (2015) 36957-36968. [10.1039/c5ra00717h](https://doi.org/10.1039/c5ra00717h)
- [130] A. Aouniti, M. El Azzouzi, I. Belfilali, I.K. Warad, H. Elmsellem, B. Hammouti, C. Jama, F. Bentiss, A. Zarrouk, Anticorrosion Potential of New Synthesized Naphtamide on Mild Steel in Hydrochloric Acid Solution: Gravimetric, Electrochemical, Surface Morphological, UV-Visible and Theoretical Investigations, *ANALYTICAL & BIOANALYTICAL ELECTROCHEMISTRY*, 10 (2018) 1193-1210
- [131] G. Bereket, E. Hür, C. Öğretir, Quantum chemical studies on some imidazole derivatives as

- corrosion inhibitors for iron in acidic medium, *Journal of Molecular Structure: THEOCHEM*, 578 (2002) 79-88. [https://doi.org/10.1016/S0166-1280\(01\)00684-4](https://doi.org/10.1016/S0166-1280(01)00684-4)
- [132] K.F. Khaled, K. Babić-Samardžija, N. Hackerman, Theoretical study of the structural effects of polymethylene amines on corrosion inhibition of iron in acid solutions, *Electrochimica Acta*, 50 (2005) 2515-2520. <https://doi.org/10.1016/j.electacta.2004.10.079>
- [133] K. Babić-Samardžija, K.F. Khaled, N. Hackerman, Investigation of the inhibiting action of O-, S- and N-dithiocarbamate(1,4,8,11-tetraazacyclotetradecane)cobalt(III) complexes on the corrosion of iron in HClO<sub>4</sub> acid, *Applied Surface Science*, 240 (2005) 327-340. <https://doi.org/10.1016/j.apsusc.2004.07.015>
- [134] L.H. Madkour, S. Kaya, C. Kaya, L. Guo, Quantum chemical calculations, molecular dynamics simulation and experimental studies of using some azo dyes as corrosion inhibitors for iron. Part 1: Mono-azo dye derivatives, *Journal of the Taiwan Institute of Chemical Engineers*, 68 (2016) 461-480
- [135] S.K. Saha, P. Ghosh, A.R. Chowdhury, P. Samanta, N. Murmu, A.K. Lohar, P. Banerjee, Corrosion control of chrome steel ball in nitric acid medium using schiff base ligand and corresponding metal complexes: a combined experimental and theoretical study, *Can Chem Trans*, 2 (2014) 381-402
- [136] M. ElBelghiti, Y. Karzazi, A. Dafali, B. Hammouti, F. Bentiss, I. Obot, I. Bahadur, E. Ebenso, Experimental, quantum chemical and Monte Carlo simulation studies of 3, 5-disubstituted-4-amino-1, 2, 4-triazoles as corrosion inhibitors on mild steel in acidic medium, *Journal of Molecular Liquids*, 218 (2016) 281-293
- [137] G. Gao, C. Liang, Electrochemical and DFT studies of β-amino-alcohols as corrosion inhibitors for brass, *Electrochimica Acta*, 52 (2007) 4554-4559. <https://doi.org/10.1016/j.electacta.2006.12.058>
- [138] L.H. Madkour, Aminic nitrogen-bearing polydentate Schiff base compounds as corrosion inhibitors for iron in acidic and alkaline media: A combined experimental and DFT studies Loutfy H. Madkour\*, SK Elroby 2, *J. Corros. Sci. Eng.*, 17 (2014).